Global variability in leaf respiration in relation to climate, plant functional types and leaf traits

Owen K. Atkin[1,2], Keith J. Bloomfield[2], Peter B. Reich[3,4], Mark G. Tjoelker[4], Gregory P. Asner[5], Damien Bonal[6], Gerhard Bönisch[7], Matt G. Bradford[8], Lucas A. Cernusak[9], Eric G. Cosio[10], Danielle Creek[2,4], Kristine Y. Crous[2,4], Tomas F. Domingues[11], Jeffrey S. Dukes[12,13], John J. G. Egerton[2], John R. Evans[2], Graham D. Farquhar[2], Nikolaos M. Fyllas[14], Paul P. G. Gauthier[2,15], Emanuel Gloor[16], Teresa E. Gimeno[4], Kevin L. Griffin[17], Rossella Guerrieri[18,19], Mary A. Heskel[2], Chris Huntingford[20], Françoise Yoko Ishida[9], Jens Kattge[7], Hans Lambers[21], Michael J. Liddell[22], Jon Lloyd[9,23], Christopher H. Lusk[24], Roberta E. Martin[5], Ayal P. Maksimov[25], Trofim C. Maximov[25], Yadvinder Malhi[26], Belinda E. Medlyn[27,4], Patrick Meir[2,18], Lina M. Mercado[28,20], Nicholas Mirotchnick[29], Desmond Ng[2,30], Ülo Niinemets[31], Odhran S. O'Sullivan[2], Oliver L. Phillips[16], Lourens Poorter[32], Pieter Poot[21], I. Colin Prentice[27,23], Norma Salinas[10,26], Lucy M. Rowland[18], Michael G. Ryan[33], Stephen Sitch[28], Martijn Slot[34,35], Nicholas G. Smith[13], Matthew H. Turnbull[36], Mark C. VanderWel[34,37], Fernando Valladares[38], Erik J. Veneklaas[21], Lasantha K. Weerasinghe[2,39], Christian Wirth[40], Ian J. Wright[27], Kirk R. Wythers[3], Jen Xiang[1,2], Shuang Xiang[2,41] and Joana Zaragoza-Castells[18,28]

[1]ARC Centre of Excellence in Plant Energy Biology, Research School of Biology, The Australian National University, Building 134, Canberra, ACT 0200, Australia; [2]Division of Plant Sciences, Research School of Biology, The Australian National University, Building 46, Canberra, ACT 0200, Australia; [3]Department of Forest Resources, University of Minnesota, 1530 Cleveland Avenue North, St Paul, MN 55108, USA; [4]Hawkesbury Institute for the Environment, University of Western Sydney, Penrith, NSW 2751, Australia; [5]Department of Global Ecology, Carnegie Institution for Science, Stanford, CA 94305, USA; [6]INRA, UMR 1137 Ecologie et Ecophysiologie Forestières, Champenoux 54280, France; [7]Max-Planck-Institute for Biogeochemistry, P07745 Jena, Germany; [8]CSIRO Land and Water, Tropical Forest Research Centre, Atherton, Qld, Australia; [9]School of Marine and Tropical Biology and Centre for Tropical Environmental and Sustainability Science, James Cook University, Cairns, Qld, Australia; [10]Pontificia Universidad Católica del Perú, Seccion Quimica, Av Universitaria 1801, San Miguel, Lima, Peru; [11]Faculdade de Filosofia Ciências e Letras de Ribeirão Preto, Universidade de São Paulo, Sao Paulo, Brazil; [12]Department of Forestry and Natural Resources, Purdue University, 715 West State Street, West Lafayette, IN 47907, USA; [13]Department of Biological Sciences, Purdue University, 915 West State Street, West Lafayette, IN 47907, USA; [14]Department of Ecology and Systematics, Faculty of Biology, National and Kapodistrian University of Athens, Athens 15784, Greece; [15]Department of Geosciences, Princeton University, Guyot Hall, Princeton, NJ 08544, USA; [16]School of Geography, University of Leeds, Woodhouse Lane, Leeds, LS9 2JT, UK; [17]Department of Earth and Environmental Sciences, Lamont-Doherty Earth Observatory, Columbia University, Palisades, NY 10964-8000, USA; [18]School of Geosciences, University of Edinburgh, Edinburgh, EH9 3JN, UK; [19]Earth Systems Research Center, University of New Hampshire, Morse Hall, 8 College Road, Durham, NH 03824, USA; [20]Centre for Ecology and Hydrology, Wallingford, OX10 8BB, UK; [21]School of Plant Biology, The University of Western Australia, Crawley, Perth, WA 6009, Australia; [22]Discipline of Chemistry & Centre for Tropical Environmental and Sustainable Sciences, James Cook University, Cairns, Qld, Australia; [23]Department of Life Sciences, Imperial College London, Silwood Park Campus, Ascot, SL5 7PY, UK; [24]Department of Biological Sciences, University of Waikato, Private Bag, 3105, Hamilton, New Zealand; [25]Institute for Biological Problems of Cryolithozone Siberian Branch RAS (IBPC), Yakutsk, Russia; [26]Environmental Change Institute, School of Geography and the Environment, University of Oxford, South Parks Road, Oxford, OX1 3QY, UK; [27]Department of Biological Sciences, Macquarie University, Sydney, NSW 2109, Australia; [28]Geography, College of Life and Environmental Sciences, University of Exeter, Amory Building, Exeter, EX4 4RJ, UK; [29]Department of Ecology and Evolutionary Biology, University of Toronto, 25 Willcocks Street, Toronto, ON M5S 3B2, Canada; [30]National Parks Board HQ, Singapore Botanic Gardens, 1 Cluny Road, Singapore city 259569, Singapore; [31]Department of Plant Physiology, Estonian University of Life Sciences, Kreutzwaldi 1, 51014 Tartu, Estonia; [32]Forest Ecology and Forest Management Group, Wageningen University, PO Box 47, 6700AA Wageningen, the Netherlands; [33]Natural Resource Ecology Laboratory, Colorado State University, Fort Collins, CO 80523, USA; [34]Department of Biology, University of Florida, Gainesville, FL 32611, USA; [35]Smithsonian Tropical Research Institute, Apartado 0843-03092, Balboa, Republic of Panama; [36]Centre for Integrative Ecology, School of Biological Sciences, University of Canterbury, Private Bag 4800, Christchurch, New Zealand; [37]Department of Biology, University of Regina, 3737 Wascana Pkwy, Regina, SK S4S 3M4, Canada; [38]Laboratorio Internacional de Cambio Global (LINC-Global), Museo nacional de Ciencias Naturales, MNCN, CSIC, Serrano 115 dpdo, E-28006 Madrid, Spain; [39]Faculty of Agriculture, University of Peradeniya, Peradeniya 20400, Sri Lanka; [40]Institut für Spezielle Botanik und Funktionelle Biodiversität, Universität Leipzig, Johannisallee 21, 04103 Leipzig, Germany; [41]Chengdu Institute of Biology, Chinese Academy of Sciences, No. 9, Section 4, Renmin South Road, Chengdu, Sichuan 610041, China

Author for correspondence:
Owen K. Atkin
Tel +61 0 2 6125 5046
Email: Owen.Atkin@anu.edu.au

Summary

• Leaf dark respiration (R_{dark}) is an important yet poorly quantified component of the global carbon cycle. Given this, we analyzed a new global database of R_{dark} and associated leaf traits.

• Data for 899 species were compiled from 100 sites (from the Arctic to the tropics). Several woody and nonwoody plant functional types (PFTs) were represented. Mixed-effects models were used to disentangle sources of variation in R_{dark}.

• Area-based R_{dark} at the prevailing average daily growth temperature (T) of each site increased only twofold from the Arctic to the tropics, despite a 20°C increase in growing T (8–28°C). By contrast, R_{dark} at a standard T (25°C, R_{dark}^{25}) was threefold higher in the Arctic than in the tropics, and twofold higher at arid than at mesic sites. Species and PFTs at cold sites exhibited higher R_{dark}^{25} at a given photosynthetic capacity (V_{cmax}^{25}) or leaf nitrogen concentration ([N]) than species at warmer sites. R_{dark}^{25} values at any given V_{cmax}^{25} or [N] were higher in herbs than in woody plants.

• The results highlight variation in R_{dark} among species and across global gradients in T and aridity. In addition to their ecological significance, the results provide a framework for improving representation of R_{dark} in terrestrial biosphere models (TBMs) and associated land-surface components of Earth system models (ESMs).

Introduction

A challenge for the development of terrestrial biosphere models (TBMs) and associated land surface components of Earth system models (ESMs) is improving representation of carbon (C) exchange between terrestrial plants and the atmosphere, and incorporating biological variation arising from diversity in plant functional types (PFTs) and climate (Sitch *et al.*, 2008; Booth *et al.*, 2012; Prentice & Cowling, 2013; Fisher *et al.*, 2014). Accounting for patterns in leaf respiratory CO_2 release in darkness (R_{dark}) in TBMs and ESMs is crucial (King *et al.*, 2006; Huntingford *et al.*, 2013; Wythers *et al.*, 2013), as plant respiration – roughly half of which comes from leaves (Atkin *et al.*, 2007) – releases *c.* 60 Pg C yr^{-1} (Prentice *et al.*, 2001; Canadell *et al.*, 2007; IPCC, 2013). Fractional changes in leaf R_{dark} as a consequence of climate change can, therefore, have large impacts on simulated net C exchange and C storage for individual ecosystems (Piao *et al.*, 2010) and, by influencing the CO_2 concentration of the atmosphere, potentially feedback so as to alter the extent of future global warming (Cox *et al.*, 2000; Huntingford *et al.*, 2013). There is growing acceptance, however, that leaf R_{dark} is not adequately represented in TBMs and ESMs (Huntingford *et al.*, 2013; Smith & Dukes, 2013), resulting in substantial uncertainty in future climate predictions (Leuzinger & Thomas, 2011); consequently, there is a need to improve representation of leaf R_{dark} in predictions of future vegetation–climate interactions for a range of possible fossil fuel-burning scenarios (Atkin *et al.*, 2014). Achieving this requires an analysis of variation in leaf R_{dark} along global climate gradients and among taxa within ecosystems; and establishing whether relationships between leaf R_{dark} and associated leaf traits vary predictably among environments and PFTs (Wright *et al.*, 2004, 2006; Reich *et al.*, 2006; Atkin *et al.*, 2008). PFTs enable a balance to be struck between the computational requirements of TBMs to minimize the number of plant groups and availability of sufficient data to fully characterize functional types, and the reality that plant species differ widely in trait values. Most TBMs contain at least five PFTs, with species being organized on the basis of canopy characteristics such as leaf size and life span, physiology, leaf mass-to-area ratio, canopy height and phenology (Fisher *et al.*, 2014). Although classifications that are directly trait-based are emerging (Kattge *et al.*, 2011), PFT classifications are still widely used in TBMs and land surface components of ESMs. As such, discerning the role of PFTs in modulating relationships between leaf R_{dark} and associated leaf traits will provide critical insights.

Although our understanding of global variation in leaf R_{dark} remains inadequate, it is known that, in natural ecosystems, rates vary markedly within and among species, and among PFTs. Surveys of leaf R_{dark} at a common temperature (T) of 25°C (R_{dark}^{25}) allow standardized comparisons of respiratory capacity (and associated investment in mitochondrial protein) to be made among contrasting sites and species. In a survey of 20 sites around the world, Wright *et al.* (2006) reported a 16-fold variation in mass-based leaf R_{dark}^{25}. Importantly, much of the variation in rates of R_{dark}^{25} is present within sites among co-occurring species and PFTs, reflecting strong genetic (as opposed to environmental) control of respiratory flux, as demonstrated by interspecific comparisons in controlled environments (Reich *et al.*, 1998b; Loveys *et al.*, 2003; Xiang *et al.*, 2013) and field conditions (Bolstad *et al.*, 2003; Tjoelker *et al.*, 2005; Turnbull *et al.*, 2005; Slot *et al.*, 2013). Differences in demand for respiratory products (e.g. ATP, reducing equivalents and/or C skeletons) from metabolic processes (such as photosynthesis (A), phloem loading, nitrogen (N) assimilation and protein turnover) underpin genotype variations in leaf R_{dark} (Lambers, 1985; Bouma *et al.*, 1994, 1995; Noguchi & Yoshida, 2008). Consequently, interspecific variations in leaf R_{dark} often scale with photosynthesis (Gifford, 2003; Wright *et al.*, 2004; Campbell *et al.*, 2007) and leaf [N] (Ryan, 1995; Reich *et al.*, 1998a). Importantly, $R_{dark} \leftrightarrow$ [N] relationships differ among PFTs, with R_{dark} at a given [N] being higher in forbs than in woody angiosperms and gymnosperms (Reich *et al.*, 2008).

Any analysis of global patterns of leaf R_{dark} must consider the impacts of the environment on respiratory metabolism; here, the impact of T on R_{dark} is of particular interest. Leaf R_{dark} is sensitive to short-term (scale of minutes) changes in T (Wager, 1941; Atkin & Tjoelker, 2003; Kruse *et al.*, 2011), with the sensitivity declining as leaf T increases (Tjoelker *et al.*, 2001). With sustained changes in the prevailing ambient growth T, leaf R_{dark}

often acclimates to the new conditions (Tjoelker *et al.*, 2009; Ow *et al.*, 2010; Dillaway & Kruger, 2011; Slot *et al.*, 2014a), resulting in higher rates of R_{dark}^{25} in cold-acclimated plants (Larigauderie & Körner, 1995; Atkin & Tjoelker, 2003). Such acclimation can occur as quickly as within one to a few days (Atkin *et al.*, 2000) and can result in leaf R_{dark} measured at the prevailing ambient T (R_{dark}^{amb}) being nearly identical (i.e. near-homeostatic) in thermally contrasting environments (Zaragoza-Castells *et al.*, 2008). Another factor that can influence leaf R_{dark} is drought, with rates declining following the onset of drought (Flexas *et al.*, 2005; Ayub *et al.*, 2011; Crous *et al.*, 2011). However, the response to drought can vary, with other studies reporting no change (Gimeno *et al.*, 2010) or an increase in R_{dark}^{25} with increasing drought (Bartoli *et al.*, 2005; Slot *et al.*, 2008; Metcalfe *et al.*, 2010). Thus, while exposure to hot growth conditions is invariably associated with a decline in R_{dark}^{25}, there is as yet no clear consensus on how differences in water availability across sites impact on R_{dark}^{25}.

As noted earlier, an overview of global variations in R_{dark} is needed to provide benchmarking data to constrain and test alternative representations of autotrophic respiratory CO_2 release in TBMs and the land surface components of ESMs. The data reported by Wright *et al.* (2006) represent the largest compilation to date, having compared mass-based rates of leaf R_{dark} in 208 woody and 60 herb/grass species from 20 contrasting sites, mostly in temperate regions. However, no data were available for plants growing in upland tropical or Arctic ecosystems. Nevertheless, several interesting phenomena were identified, including the fact that rates of R_{dark}^{25} (and $R_{dark}^{25} \leftrightarrow$[N] relationships) were similar at sites that differ in growth T; a similar result was reported in an earlier analysis by Reich *et al.* (1998a). This observation contrasts with earlier studies that reported higher R_{dark} at a standard measurement T in plants growing at colder sites (Stocker, 1935; Wager, 1941; Semikhatova *et al.*, 2007), consistent with thermal acclimation responses of respiratory metabolism (Atkin & Tjoelker, 2003). A new global database not only requires rates of R_{dark}^{25} and R_{dark}^{amb}, but also values of other leaf traits currently used in TBMs to predict respiration.

While there is no single approach to estimating leaf R_{dark} in TBMs – Schwalm *et al.* (2010) reported 15 unique approaches from 21 TBMs – it is common for R_{dark} to be related to gross primary productivity (GPP), either directly as a fraction of GPP or indirectly as a fraction of maximum carboxylation capacity, with GPP estimated from enzyme kinetic or stomatal conductance (g_s) models. Other models estimate leaf R_{dark} from other traits, including [N] (e.g. Biome-BGC; Thornton *et al.*, 2002) and/or vegetation C (Lund–Postdam–Jena model (LPJ); Sitch *et al.*, 2003). In the UK Hadley Centre model JULES (Joint UK Land Environment Simulator; Clark *et al.*, 2011), R_{dark}^{25} is assumed to be proportional to photosynthetic carboxylation capacity at 25°C (V_{cmax}^{25}), with V_{cmax}^{25} predicted from PFT-dependent values of leaf [N] according to a single $V_{cmax}^{25} \leftrightarrow$[N] relationship (Schulze *et al.*, 1994; Cox *et al.*, 1998); JULES also provides the opportunity to link terrestrial C cycling to climate prediction. However, as with other models linking R_{dark}^{25} to GPP, JULES does not account for climate or PFT-dependent

variations in $R_{dark}^{25} \leftrightarrow V_{cmax}^{25} \leftrightarrow$[N] relationships. A new global database will enable assessment of $R_{dark}^{25} \leftrightarrow V_{cmax}^{25} \leftrightarrow$[N] (and phosphorus concentrations, [P]) relationships, both among PFTs and along climate gradients.

Here, using published and unpublished data (Supporting Information Tables S1, S2), we report on a newly compiled global leaf R_{dark} and associated traits (GlobResp) database. The GlobResp database increases biogeographical and phylogenetic coverage compared with earlier data sets, and contains information on leaf R_{dark} and associated leaf traits for 899 species from 100 sites. We used the GlobResp database to address the following questions. First, do rates of R_{dark} at prevailing ambient T (R_{dark}^{amb}) and at a standardized reference T of 25°C (R_{dark}^{25}) vary with climate across sites in relation to T (i.e. thermal environment) and aridity. Secondly, are the observed patterns consistent with hypotheses concerning thermal acclimation and adaptation (i.e. evolutionary response resulting from genetic changes in populations and taxa) of R_{dark}? And thirdly, does scaling between leaf R_{dark} and associated leaf traits vary among environments and PFTs? Finally, a key aim of our study was to predict global variability in R_{dark}^{25} from a group of independent input variables, using data on corresponding leaf traits, climate or a combination of traits and climate; here our aim was to provide equations that would facilitate improved representation of leaf R_{dark} in TBMs and associated land surface components of ESMs.

Materials and Methods

Compilation of a global database

To create a global leaf respiration and associated leaf traits (GlobResp) database, we combined data from recent field campaigns (Table S1) with previously published data (Table S2). Data were obtained from recent publications (Atkin *et al.*, 2013; Slot *et al.*, 2013, 2014b; Weerasinghe *et al.*, 2014) and the TRY trait database (Kattge *et al.*, 2011) that included published studies (Mooney *et al.*, 1983; Oberbauer & Strain, 1985, 1986; Chazdon & Kaufmann, 1993; Kamaluddin & Grace, 1993; Kloeppel *et al.*, 1993; García-Núñez *et al.*, 1995; Kloeppel & Abrams, 1995; Zotz & Winter, 1996; Grueters, 1998; Miyazawa *et al.*, 1998; Reich *et al.*, 1998a; Bolstad *et al.*, 1999; Craine *et al.*, 1999; Mitchell *et al.*, 1999; Niinemets, 1999; Wright *et al.*, 2001, 2004, 2006; Meir *et al.*, 2002, 2007; Wright & Westoby, 2002; Veneklaas & Poot, 2003; Tjoelker *et al.*, 2005; Machado & Reich, 2006; Poorter & Bongers, 2006; Swaine, 2007; Sendall & Reich, 2013). The combined database contains data from 100 thermally contrasting sites (899 species representing 136 families, and *c.* 1200 species–site combinations) from biomes ranging from 69°N to 43°S and from sea level to 3450 m above sea level (asl) (Fig. 1a; Tables 1, 2).

A wide range of terrestrial biomes is represented in the new combined GlobResp database (Table 1) along with most of the PFTs categorized in JULES – a land surface component of an ESM framework (Clark *et al.*, 2011) – and in LPJ, representing a model with a greater diversity of PFTs from the wider TBM community (Sitch *et al.*, 2003) (Table 2). Users who would like
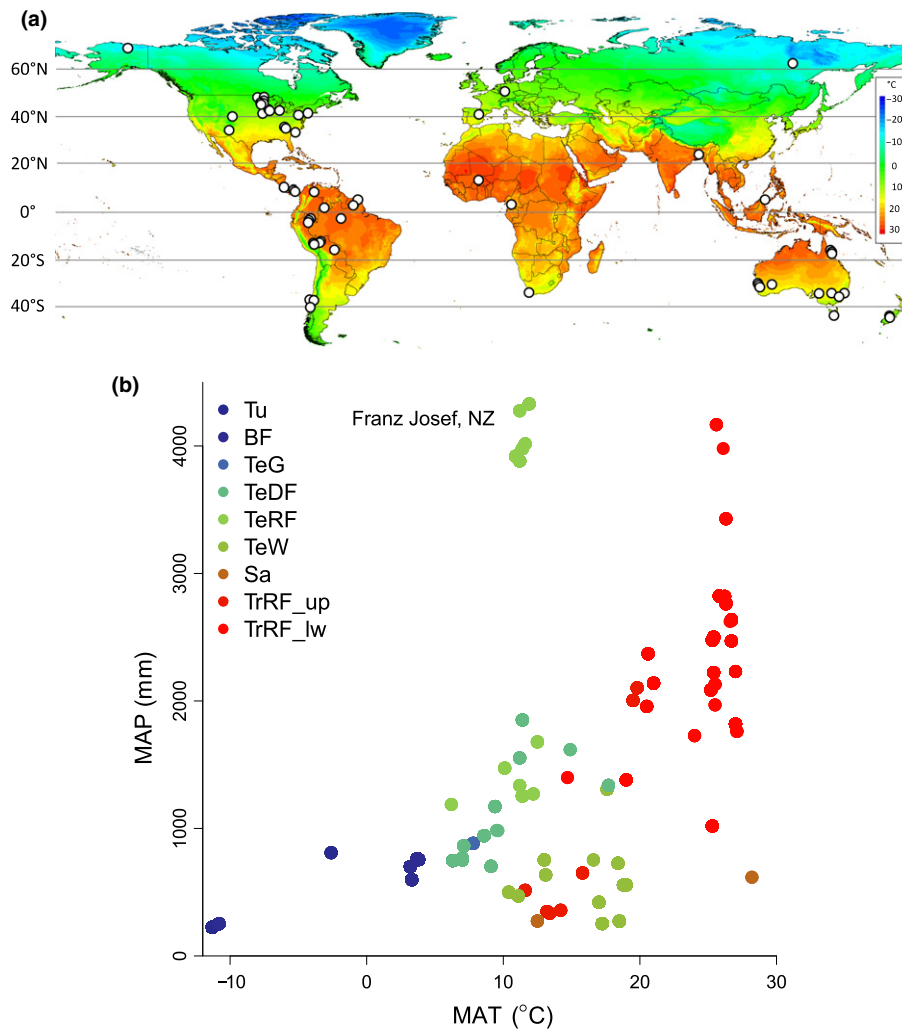
Fig. 1 Location and climate envelope of the sites at which leaf dark respiration (R_{dark}) and associated traits were measured. (a) Site locations on a global map showing spatial variability in mean annual temperature (MAT); (b) plot of mean annual precipitation (MAP) vs MAT for each site (shown in biome classes). See Table 1 for summary of site information, and Tables S1 and S2 for details on the latitude, longitude, altitude (height above sea level; asl), MAT, mean temperature of the warmest quarter (i.e. warmest 3-month period yr^{-1}; TWQ), MAP, mean precipitation of the warmest quarter (PWQ), and aridity index (AI, ratio of MAP to mean annual potential evapotranspiration, PET). In (b), biome categorization of each site is shown: Tu, tundra; BF, boreal forest; TeDF, temperate deciduous forest; TeRF, temperate rainforest; TeW, temperate woodland; Sa, savanna; TrRF_up, upland tropical rainforest (> 1500 m asl); TrRF_low, lowland tropical rainforest (< 1500 m asl). In (b), note the unusually high MAP at the Franz Josef TeRF site on the South Island of New Zealand (NZ).

to use GlobResp (to be available via the TRY trait database) will also be provided with species classified according to other PFT schemes (including the Sheffield dynamic global vegetation model; Woodward *et al.*, 1998). Several PFTs, however, remain poorly represented in GlobResp: plants that use the C$_4$ photosynthetic pathway, boreal deciduous needle-leaved trees (BorDcNl) and tropical herbs/grasses (TrpH – which in the database includes a mixture of species that use either C$_3$ or C$_4$ pathways of photosynthesis). Lianas are not yet included in PFT classifications of global TBMs, and are also absent from GlobResp, although some data are now emerging for a limited number of sites (Slot *et al.*, 2013). The GlobResp database was limited to field-collected data from sites where climate data could be attributed. We excluded data from controlled-environment experiments (e.g. growth cabinets and glasshouses), as well as experiments where atmospheric CO$_2$, temperature, irradiance,

nutrient supply and/or water supply were manipulated. For each site, long-term climate data were obtained from the WorldClim climate database for the years 1960–1990, at a resolution of 30 arc s, or 1 km at the equator (Hijmans *et al.*, 2005). Aridity indices (AIs, ratio of mean annual precipitation (MAP) to potential evapotranspiration (PET), and hence a lower value of AI indicates more arid conditions) at each site were estimated according to Zomer *et al.* (2008) using the CGIAR-CSI Global-PET database (http://www.cgiar-csi.org).

Mean temperature of the warmest quarter (i.e. warmest 3-month period yr^{-1}; TWQ) and measuring month (MMT, mean temperature of the month when respiration data were recorded) were used to characterize the growth T at each site. Records of the actual measuring month, required to estimate MMT, were only available for half the sites. Consequently, we used TWQ as a measure of the growth T, as most temperate and

Table 1 Sample sites and climate conditions at which leaf dark respiration (R_{dark}) was measured

Country-region	Biomes	Altitude (m asl)	MAT (°C)	TWQ (°C)	MAP (mm)	PWQ (mm)	AI	No. of species	PFTs present (JULES)
USA-AK	Tu	720	−11.3	8.2	225	113	0.61	37	BlT, C3H, S
Russia-Siberia	BF	217	−10.8	15.4	254	122	0.46	3	BlT, NlT
USA-CO	Tu	3360	−2.6	7.5	811	203	1.20	10	BlT, C3H, NlT, S
USA-MN	BF, TeDF, TeG	365	4.4	18.4	735	303	0.87	53	BlT, C3H, C4H, NlT, S
USA-IA	TeDF	385	7.1	20.2	865	315	0.83	11	BlT, NlT
USA-WI	TeDF, TeG	293	7.7	20.6	880	315	0.93	15	BlT, C3H, NlT
USA-MI	TeDF	200	8.6	19.9	944	268	0.98	1	NlT
Germany	TeDF	60	9.1	17.2	704	190	0.92	9	BlT, NlT
USA-NY	TeDF	225	9.4	20.8	1173	308	1.20	3	BlT
USA-PA	TeDF	355	9.5	19.9	915	262	0.91	3	BlT
Spain	TeW	1017	10.7	19.2	487	99	0.48	1	BlT
Australia-TAS	TeRF	144	11.0	14.7	1325	211	1.58	14	BlT, S
Chile	TeRF	434	11.1	15.4	1467	103	1.40	18	BlT, NlT
USA-TN	TeDF	775	11.2	20.1	1554	389	1.34	13	BlT, C3H, NlT, S
New Zealand	TeRF	202	11.3	15.9	4014	1011	4.50	16	BlT, NlT, S
USA-NC	TeDF	850	11.4	20.0	1852	444	1.52	15	BlT, NlT
USA-NM	Sa	1620	12.5	22.2	275	127	0.19	9	BlT, NlT, S
Australia-ACT	TeW	572	13.0	20.7	722	271	0.58	6	BlT, NlT, S
Japan	TeDF	20	14.9	23.7	1619	433	1.92	4	BlT
South Africa	TeW	600	16.6	21.0	754	67	0.57	5	BlT, S
Peru-Andes	TrRF_up	2380	16.7	17.7	1297	373	0.79	82	BlT, C3H
Australia-SA	TeW	35	17.3	23.6	255	52	0.17	10	BlT, C3H, S
Australia-NSW	TeW	140	17.3	23.2	820	215	0.29	70	BlT, C3H, C4H, NlT, S
USA-SC	TeDF	3	17.7	25.8	1339	469	1.02	10	BlT, C3H, NlT, S
Australia-WA	TeW	204	18.7	24.5	463	47	0.32	55	BlT, C3H, S
Australia-FNQ	TrRF_lw	513	22.4	25.1	1990	934	1.35	45	BlT, S
Cameroon	TrRF_lw	550	24.0	24.8	1729	417	1.13	6	BlT, C3H
Venezuela	TrRF_lw	492	24.4	24.7	3092	693	1.61	10	BlT, S
Bolivia	TrRF_lw	400	25.3	27.0	1020	436	0.57	50	BlT
Suriname	TrRF_lw	215	25.4	26.3	2224	165	1.37	25	BlT, C3H, C4H, S
Peru-Amazon	TrRF_lw	164	25.4	26.2	2567	828	1.50	214	BlT, S
Bangladesh	TrRF_lw	21	25.5	28.5	1970	736	1.34	1	BlT
Costa Rica	TrRF_lw	135	25.7	26.7	4141	747	2.64	2	BlT, S
French Guiana	TrRF_lw	21	25.8	26.2	2824	222	1.88	70	BlT
Malaysia-Borneo	TrRF_lw	20	26.7	27.1	2471	501	1.64	29	BlT, S
Brazil-Amazon	TrRF_lw	115	27.0	27.6	2232	401	1.39	9	BlT
Panama	TrRF_lw	98	27.0	27.7	1822	300	1.19	18	BlT
Niger	Sa	280	28.2	31.4	618	55	0.30	3	BlT, S

Sites are shown in order of increasing mean annual temperature (MAT). Where multiple sites were found within a region, values represent the mean values of all sites, weighted for the number of species at each site (see Tables S1 and S2 for further details). Data on climate are from the WorldClim database (Hijmans *et al.*, 2005). The number of species measured at each site is shown, as is the number of observational rows of data contained in the GlobResp database. For the latter, an observational row represents individual measurements for all unpublished data (see Table S1), while for published data (Table S2) observational rows in many cases represent mean values of species–site combinations. Joint UK Land Environment Simulator (JULES; Clark *et al.*, 2011) plant functional types (PFTs) at each site shown, according to: BlT, broadleaved tree; C3H, C_3 metabolism herb/grass; C4H, C_4 metabolism herb/grass; NlT, needle-leaved tree; S, shrub. Biome classes: BF, boreal forests; TeDF, temperate deciduous forest; TeG, temperate grassland; TeRF, temperate rainforest; TeW, temperate woodland; TrRF_lw, lowland tropical rainforest (< 1500 m above sea level; asl); TrRF_up, upland tropical rainforest (>1500 m asl); Tu, tundra. TWQ, mean temperature of the warmest quarter (i.e. warmest 3-month period yr^{-1}); MAP, mean annual precipitation; PWQ, mean precipitation of the warmest quarter; AI, aridity index, calculated as the ratio of MAP to mean annual potential evapotranspiration (UNEP, 1997; Zomer *et al.*, 2008). Australia/ACT, Australian Capital Territory; Australia/FNQ, Far North Queensland; Australia-NSW, New South Wales; Australia-TAS, Tasmania; Australia-WA, Western Australia; USA-AK, Alaska; USA-CO, Colorado; USA-MN, Minnesota; USA-IA, Iowa; USA-WI, Wisconsin; USA-MI, Michigan; USA-PA, Pennsylvania; USA-NY, New York; USA-NC, North Carolina; USA-TN, Tennessee; USA-NM, New Mexico; USA-SC, South Carolina.

Arctic sites were sampled in summer, which corresponded with the warmest quarter. For tropical sites we also used TWQ, although seasonal *T* variation is comparatively low in tropical regions (Archibold, 1995).

Data were collected using similar protocols described herein (Methods S1) and in published works (Table S2). Outer canopy leaves were sampled early to mid-morning, kept in moist, dark conditions, with R_{dark} measured using infrared gas analyzers

following a period of dark adjustment – typically 30–45 min (Azcón-Bieto *et al.*, 1983; Atkin *et al.*, 1998). Only data from mature, fully expanded leaves were included; as such, R_{dark} did not reflect the metabolic demands of biosynthesis associated with localized cell division/expansions processes. Rather, the measured rates of R_{dark} probably reflected demands for respiratory products associated with cellular maintenance, and potentially phloem loading (Amthor, 2000). We note that the daytime measured

Table 2 Details of plant functional types (PFTs) contained in the GlobResp database

ESM framework	PFTs	No. of sites	Minimum latitude	Maximum latitude	No. of species
JULES	BlT	94	−43.42	68.63	642
	C3H	14	−34.04	68.63	75
	C4H	3	−33.84	45.41	8
	NlT	20	−43.31	62.25	24
	S	32	−43.42	68.63	124
LPJ	BorDcBl	10	40.05	68.63	18
	BorDcNl	3	33.33	62.25	2
	BorEvNl	6	40.05	62.25	10
	TmpDcBl	25	−43.41	50.60	46
	TmpEvBl	33	−43.42	68.63	193
	TmpEvNl	13	−43.31	50.60	18
	TmpH	12	−34.04	68.63	79
	TrpDcBl	20	−15.78	13.20	50
	TrpEvBl	39	−17.68	24.20	468
	TrpH	3	−13.11	3.38	4

PFTs for two Earth system model (ESM) frameworks are shown: Joint UK Land Environment Simulator (JULES; Clark *et al.*, 2011) and Lund–Post-dam–Jena model (LPJ; Sitch *et al.*, 2003). For each PFT, the number of field sites and species are shown, as is the maximum absolute latitude and longitude of the PFT distribution. For JULES, the following PFTs are shown: BlT, broad-leaved tree; C3H, C_3 metabolism herb/grass; C4H, C_4 metabolism herb/grass; NlT, needle-leaved tree; S, shrub. For LPJ, the following PFTs are shown: BorDcBl, boreal deciduous broadleaved tree/shrub; BorDcNl, boreal deciduous needle-leaved tree/shrub; BorEvNl, boreal evergreen needle-leaved tree/shrub; TmpDcBl, temperate deciduous broadleaved tree/shrub; TmpEvBl, temperate evergreen broadleaved tree/shrub; TmpEvNl, temperate evergreen needle-leaved tree/shrub; TmpH, temperate herb/grass; TrpDcBl, tropical deciduous broadleaved tree/shrub; TrpEvBl, tropical evergreen broadleaved tree/shrub; TrpH, tropical herb/grass. Note: in some cases, individual species occurred at multiple sites in multiple biomes. Finally, an overwhelming majority of the shrubs (S) were evergreen (123 species–site combinations) compared with deciduous shrubs (11 species–site combinations).

rates of R_{dark} may have differed from equivalent fluxes at night (when compared at an equivalent T), reflecting the potential for diel differences in substrate availability and the extent of sucrose loading.

The GlobResp database contains R_{dark} expressed per unit leaf dry mass and per unit leaf area. Where available, the database includes values of light-saturated photosynthesis (A_{sat}) and associated values of internal CO_2 concentration (C_i) and g_s, leaf mass per unit area (M_a), leaf [N] and leaf [P].

Temperature normalization of respiration rates

Leaf measurement T ranged from 6 to 40°C among sites, with most measured between 16 and 33°C (T_1 in Eqn 1). To enable comparisons of leaf R_{dark}, we calculated area- and mass-based rates both for a common temperature (25°C) and at the growth T at each site (TWQ and MMT) – see Methods S2 for further details. To estimate rates of R_{dark} (R_2) at a given T (T_2), we calculated rates of R_{dark} at 25°C ($R_{dark}{}^{25}$), TWQ ($R_{dark}{}^{TWQ}$) and MMT ($R_{dark}{}^{MMT}$) using a temperature-dependent Q_{10} (Tjoelker *et al.*, 2001) based on a known rate (R_1) at experimental T (T_1) using the equation:

$$R_2 = R_1 \left(3.09 - 0.043 \left[\frac{(T_2 + T_1)}{2} \right] \right)^{\left[\frac{T_2 - T_1}{10} \right]} \qquad \text{Eqn 1}$$

Calculations of R_{dark} at the above temperatures yielded similar rates, irrespective of whether a T-dependent Q_{10} or fixed Q_{10} was used (Fig. S1).

Calculation of photosynthetic capacity

Given our objective to assess relationships between R_{dark} and the carboxylation capacity of Rubisco (V_{cmax}), we calculated the V_{cmax} for C_3 species (i.e. excluding C_4 species) for all observations where A_{sat} and C_i values were available (Farquhar *et al.*, 1980; Niinemets, 1999; von Caemmerer, 2000); this included all of the previously unpublished data (Table S1) and much of the previously published data (Table S2). V_{cmax} values were calculated according to:

$$V_{cmax} = (A_{sat} + R_{light}) \frac{C_i + K_c[1 + O/K_o]}{C_i - \Gamma_*} \qquad \text{Eqn 2}$$

where Γ_* is the CO_2 compensation point in the absence of non-photorespiratory mitochondrial CO_2 release (36.9 µbar at 25°C), O is the partial pressure of oxygen, C_i is the intercellular CO_2 partial pressure, R_{light} is the rate of nonphotorespiratory mitochondrial CO_2 release (here assumed to be equal to R_{dark}), and K_c and K_o are the Michaelis–Menten constants (K_m) of Rubisco for CO_2 and O_2, respectively (von Caemmerer *et al.*, 1994). While the assumption that $R_{light} = R_{dark}$ is unlikely to be correct in many situations (Hurry *et al.*, 2005; Tcherkez *et al.*, 2012), estimates of V_{cmax} are largely insensitive to this assumption. We assumed K_c and K_o at 25°C to be 404 µbar and 248 mbar, respectively (von Caemmerer *et al.*, 1994; Evans *et al.*, 1994) and that K_c and K_o at the measurement T could be calculated assuming activation energies (E_a) of K_c and K_o of 59.4 and 36 kJ mol^{-1}, respectively (Farquhar *et al.*, 1980). Next, we standardized V_{cmax} to 25°C ($V_{cmax}{}^{25}$) assuming $E_a = 64.8$ kJ mol^{-1} (Badger & Collatz, 1977) according to:

$$V_{cmax25} = \frac{V_{cmax}}{\exp^{[(T-25)E_a/(298*rT)]}} \qquad \text{Eqn 3}$$

where T is the leaf temperature at which A_{sat} was measured/reported (and thus V_{cmax} initially estimated), and r is the gas constant (8.314 J K^{-1} mol^{-1}). Estimates were made for C_3 species only, as representation of C_4 plants in our database was minimal (Table 2).

For data from unpublished field campaigns (Table S1), leaf area and mass values were determined as outlined in Methods S1; for sites where leaf [N] and [P] were both reported, analyses were made using Kjeldahl acid digests (Allen, 1974). For sites where only [N] was measured, leaf samples were analyzed by mass spectrometry for total N concentration (Loveys *et al.*, 2003) (see Table S1 for further details). Details of the N and P analysis procedures used for previously published data can be found in the citations listed in Table S2. Collectively, the GlobResp database

contains *c.* 1050 species : site mean values of mass- ([N]$_m$) and area-based leaf [N] ([N]$_a$), and *c.* 735 species : site mean values of [P]$_m$ and [P]$_a$.

Data analysis

Before analyses, GlobResp data were filtered for statistical outliers. Outlying values were identified as those falling beyond a central tendency band of twice the interquartile range. Three filters were applied in sequence to each PFT class separately (using LPJ groupings to enable separation of evergreen and deciduous life histories, and because there were broadly similar numbers of observations within each LPJ PFT category compared with that of JULES, where the majority of observations were within the broadleaved tree (BlT) category). Three filters were applied in the sequence: mass-based respiration at 25°C ($R_{dark,m}{}^{25}$); area-based respiration at 25°C ($R_{dark,a}{}^{25}$); and C_i (impacting on the calculation of V_{cmax}). Whenever an outlier was identified, the entire observational row was removed from the GlobResp database. Application of these filters resulted in removal of *c.* 3% of the rows from the initial database. Where leaf traits followed an approximate log-normal distribution, such values were log$_{10}$-transformed before screening for outliers and subsequent analysis. Analyses were then conducted using trait averages for unique site–species combinations and, where noted, individual rows of data.

Bivariate regression was used to explore relationships between area- and mass-based R_{dark} and latitude, TWQ (calculated using all data), MMT (mean T of the month when R_{dark} was recorded) and/or AI. In addition, backwards-stepwise regression was used to select the best-fitting equation from a starting set of input leaf traits, climate or the combination of traits plus climate variables; parameters were chosen that exhibited variance inflation factors (VIFs) < 2.0 (i.e. minimal collinearity); *F*-to-remove criterion was used to identify best-fitting parameters. Multiple regression analyses were then conducted to estimate predictive equations for the chosen variables. The predicted residual error sum of squares (PRESS statistic) was used to provide a measure of how well each regression model predicted observed R_{dark} values. Relative contributions of leaf trait and climate variables to each regression were gauged from their standardized partial regression coefficients.

Standardized major axis (SMA) analysis was used to determine the best-fitting lines (α = 0.05) for the key relationships involving $R_{dark}{}^{25}$ both on an area and mass basis (Falster *et al.*, 2006; Warton *et al.*, 2006, 2012) We tested for differences among PFT classes (JULES) and site-based temperature bands (5°C TWQ); to facilitate visual comparison of PFTs, we chose to use the four PFTs within the JULES framework, rather than the larger number of PFTs contained in the LPJ model. Using the JULES PFTs also provided an opportunity to assess how changes in growth temperature impacted on bivariate relationships within a PFT (broadleaved trees, BlT) for which there was a large number of observations and widespread distribution. We used a mixed-effects linear model to account for variability in $R_{dark}{}^{25}$ on both area- and mass-bases. Given the

hierarchical nature of the database, the linear mixed-effects model combined fixed and random components (Zuur *et al.*, 2009). The available fixed-effects variables included PFT, leaf traits ($R_{dark}{}^{25}$, $V_{cmax}{}^{25}$, M_a, [N], [P]) and climate variables (TWQ and AI). Models were run using PFT classifications from JULES and LPJ.

All continuous explanatory leaf variables were centered on their mean values before inclusion. Collinearity among leaf variables was tested using VIFs. Model specification and validation were based on the protocols outlined in Zuur *et al.* (2009) and fitted using the nlme package (Pinheiro *et al.*, 2012). Owing to the global nature of the database, species, family and site identifiers were treated as random rather than fixed effects, placing our focus on the variation contained within these terms, rather than mean values for each phylogeny/site level. Model comparisons and the significance of fixed-effects terms were assessed using Akaike's information criterion (AIC).

Stepwise and associated multiple linear regressions were conducted using Sigmaplot Statistics v12 (Systat Software Inc., San Jose, CA, USA). All other statistical analyses and modeling were conducted using the open-sourced statistical environment 'R' (R Development Core Team, 2011).

Results

Comparison of traits among PFTs

Across the GlobResp database, M_a varied 40-fold (from 19 to 780 g m^{-2}), [N]$_a$ varied 70-fold (from 0.13 to 9.13 g m^{-2}) and [P]$_a$ varied 125-fold, from 10 to 1260 mg m^{-2}. In four out of the five JULES PFTs (i.e. needle-leaved trees, broadleaved trees, shrubs and C$_3$ herbs/grasses), ranges of each of M_a, [N]$_a$ and [P]$_a$ values were relatively similar (Figs 2, S2). C$_4$ plants were poorly represented (Table 2), and were generally omitted from subsequent analyses. On average, shrubs and needle-leaved trees exhibited greater M_a values than their broadleaved tree and C$_3$ herb/grass counterparts. By contrast, [N]$_a$ values were relatively similar among the four PFTs (excluding C$_4$ plants) (Figs 2, S2). While [P]$_a$ values were similar among broad-leaved trees, C$_3$ herbs/grasses and shrubs, concentrations were higher in needle-leaved trees.

Area- and mass-based $V_{cmax}{}^{25}$ varied markedly within the four PFTs; needle-leaved trees exhibited a narrower range of $V_{cmax}{}^{25}$ values compared with the others (Fig. 3a,c). Overall, the average values of $V_{cmax}{}^{25}$ were relatively similar among the four PFTs. By contrast, average rates of $R_{dark}{}^{25}$ differed relatively more among PFTs, being highest in C$_3$ herbs/grasses, both on an area and a mass basis (Fig. 3b,d).

Relationships between leaf traits and climate

To test whether $R_{dark}{}^{25}$ was related to growth temperature or water availability, we plotted $R_{dark}{}^{25}$ against absolute latitude, TWQ and AI (Fig. 4a–c,g–i). Against latitude (considering northern and southern hemispheres separately), area-based $R_{dark}{}^{25}$ ($R_{dark,a}{}^{25}$) exhibited a significant, positive relationship
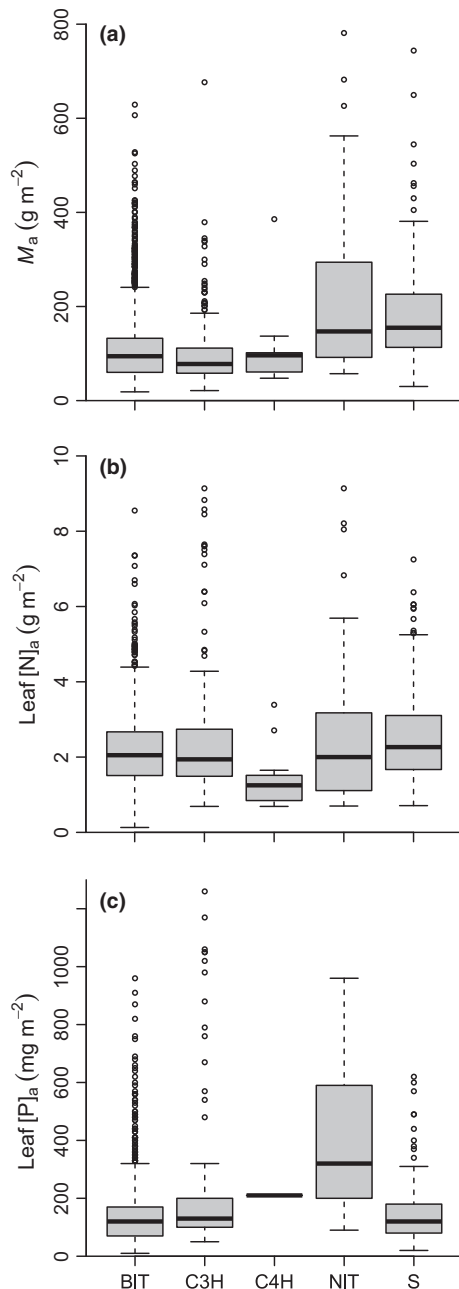
Fig. 2 Box plots showing modulation of leaf structural and chemical traits by Joint UK Land Environment Simulator (JULES; Clark *et al.*, 2011) plant functional type (PFT) classifications. Traits shown are: (a) leaf mass per unit leaf area (M_a); (b) area-based leaf nitrogen concentration ($[N]_a$); and (c) area-based leaf phosphorus concentration ($[P]_a$). Data shown are for individual row observations contained in the GlobResp database (to give an indication of underlying data distribution). The boxes indicate the interquartile range and median. Whiskers show the largest or smallest observations that fall within 1.5 times the box size; any observations outside these values are shown as individual points. Data for the following Joint UK Land Environment Simulator (JULES; Clark *et al.*, 2011) PFT classifications: BlT, broad-leaved tree; C3H, C_3 metabolism herb/grass; C4H, C_4 metabolism herb/grass; NlT, needle-leaved tree; S, shrub.

(Table 3), being threefold faster in the Arctic than at the equator (Fig. 4a), suggesting, as expected, that factors other than latitude *per se* play the key roles in determining variations in $R_{dark,m}^{25}$.

A similar pattern in the northern (but not southern) hemisphere was observed for mass-based R_{dark}^{25} (Fig. 4g; Table 3). Against TWQ, variations in $R_{dark,a}^{25}$ and $R_{dark,m}^{25}$ followed trends consistent with the latitudinal patterns, with rates being fastest at the coldest sites (Fig. 4b,h). Negative relationships were found between both area- and mass-based R_{dark}^{25} and AI (Fig. 4c,i; Table 3) – recalling that AI is lowest at the driest sites – with $R_{dark,a}^{25} \leftrightarrow$ AI markedly steeper when data from the wet cool temperate rainforest site in New Zealand were excluded (Fig. S2). Collectively, these results suggest that rates of leaf R_{dark} at 25°C are lowest at warm/moist sites near the equator, and fastest at cold/drier sites at high latitudes.

We now consider global patterns of leaf R_{dark} at the long-term average ambient growth T at each site (R_{dark}^{amb}), with R_{dark}^{amb} estimated using calculations of R_{dark} at TWQ (R_{dark}^{TWQ}) (Fig. 4d–f,j–l). In the northern hemisphere, both area- and mass-based R_{dark}^{TWQ} decreased with increasing latitude (Fig. 4d,j; Table 3). A similar pattern was observed in the southern hemisphere for mass-based but not area-based R_{dark}^{TWQ} (Fig. 4d). Both $R_{dark,a}^{TWQ}$ and $R_{dark,m}^{TWQ}$ increased with increasing TWQ (Fig. 4e,k; Table 3), indicating that rates of R_{dark}^{amb} are probably faster at the warmest sites. Similarly, the negative $R_{dark}^{TWQ} \leftrightarrow$ AI association was significant (on both an area and a mass basis; Fig. 4f,l; Table 3). However, exclusion of mass-based data from the unusually wet site in New Zealand resulted in there being no significant $R_{dark,m}^{TWQ} \leftrightarrow$ AI association (Fig. S3). Collectively, R_{dark}^{amb} (on both an area and a mass basis) was faster at the hottest sites in the tropics and mid-latitude regions. These patterns were consistent whether TWQ or MMT was used as an estimate of site-specific ambient growth T (Fig. S4).

A focus of our study was determining the best function to predict area- and mass-based R_{dark}^{25} around the globe from a group of independent input variables. Regression analysis (Table 4) shows that, based solely on leaf traits (i.e. ignoring climate), 17 and 31% of the variance in $R_{dark,a}^{25}$ and $R_{dark,m}^{25}$, respectively, was accounted for using regression equations that included leaf [N] and area : mass metrics (i.e. M_a or specific leaf area, SLA). Adding leaf [P] did little to improve the proportion of variance in R_{dark}^{25} accounted for by regression; however, [P] replaced [N] in the resultant selected equations (Table 4). By contrast, addition of V_{cmax}^{25} to the available range of leaf traits improved the r^2 of the resultant regressions (i.e. accounting for 22 and 41% of the variance in $R_{dark,a}^{25}$ and $R_{dark,m}^{25}$, respectively; Table 4). Climate parameters alone (TWQ, PWQ and/or AI) accounted for only 9–17% of variance in R_{dark}. However, combining climate with leaf traits accounted for 35 and 50% of the variance in $R_{dark,a}^{25}$ and $R_{dark,m}^{25}$, respectively (Table 4), with M_a, TWQ, V_{cmax}^{25}, rainfall/aridity and leaf [P] contributing to variance in R_{dark}, largely in that order. Replacing [P] with [N] had little effect on the r^2 of the resultant linear regressions. Thus, analysis using multiple linear regression strongly suggests that variations in leaf R_{dark} are tied to related variations in leaf structure, chemistry, and photosynthetic capacity, the thermal environment in the period during which R_{dark} measurements were made, and the average water availability.
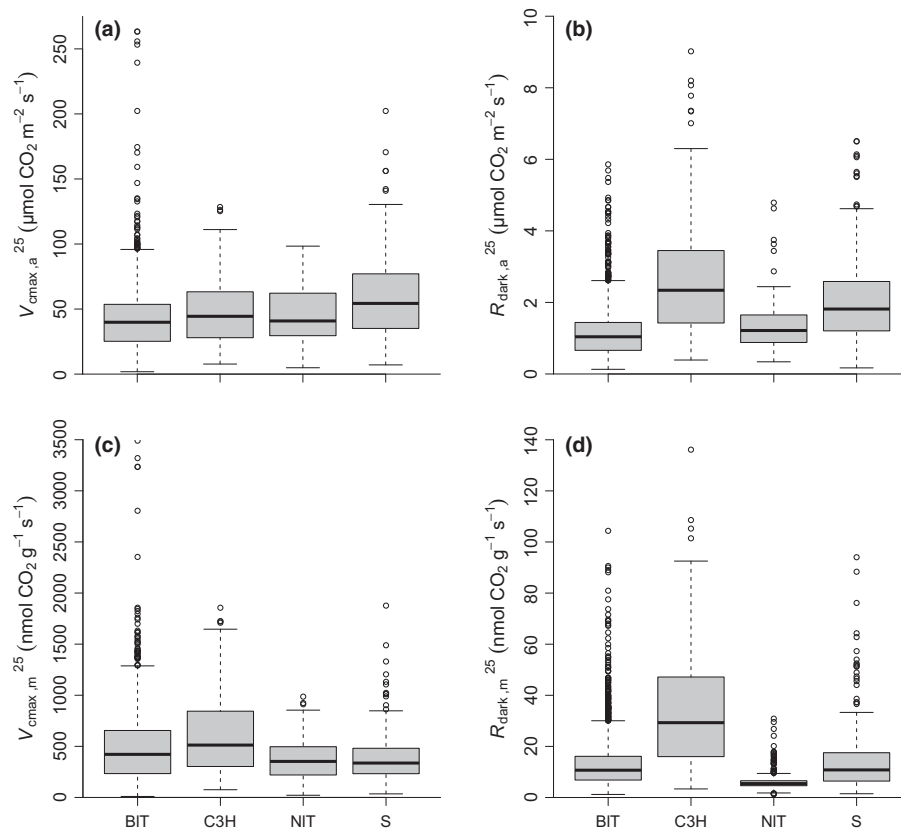
Fig. 3 Box plots showing modulation of carboxylation capacity of Rubisco (V_{cmax}) and leaf respiration in darkness (R_{dark}) by Joint UK Land Environment Simulator (JULES; Clark *et al.*, 2011) plant functional type (PFT) classifications. Data shown are for individual row observations contained in the GlobResp database (to give an indication of underlying data distribution). Rates at 25°C are shown. Traits shown are area- ($V_{cmax,a}^{25}$) (a) and mass-based ($V_{cmax,m}^{25}$) (c) carboxylation rates; and area- ($R_{dark,a}^{25}$) (b) and mass-based ($R_{dark,m}^{25}$) (d) respiration rates. Values of V_{cmax} at 25°C were calculated according to Farquhar *et al.* (1980), assuming an activation energy (E_a) of 64.8 kJ mol^{-1}. Values of R_{dark} at 25°C were calculated assuming a T-dependent Q_{10} (Tjoelker *et al.*, 2001) and eqn 7 described in Atkin *et al.* (2005). The boxes indicate the interquartile range and median. Whiskers show the largest or smallest observations that fall within 1.5 times the box size; any observations outside these values are shown as individual points. Data are for the following JULES (Clark *et al.*, 2011) PFT classifications: BlT, broadleaved tree; C3H, C$_3$ metabolism herb/grass; NlT, needle-leaved tree; S, shrub. Data are not shown for C$_4$ metabolism herbs/grasses, because of limited availability.

Relationships among PFTs

For the $R_{dark,a}^{25} \leftrightarrow V_{cmax,a}^{25}$ association, tests for common slopes revealed no significant differences among the four JULES PFTs; the elevations of those common slopes did not differ either, except for C$_3$ herbs/grasses, which exhibited faster rates of $R_{dark,a}^{25}$ at a given $V_{cmax,a}^{25}$ compared with the other PFTs (Fig. 5a). Among TWQ classes, there were also no significant differences in slopes, but the elevation (i.e. *y*-axis intercept) of the relationships differed systematically when considering all PFTs collectively (Fig. 5b), and broad-leaved trees alone (Fig. 5c). With respect to the effect of TWQ on $R_{dark,a}^{25} \leftrightarrow V_{cmax,a}^{25}$ relationships, the elevation was similar for the three highest TWQ classes (15–20, 20–25 and > 25°C), whereas $R_{dark,a}^{25}$ at any given $V_{cmax,a}^{25}$ was significantly faster at the two lowest TWQ classes (Fig. 5b; Table S3). A similar pattern emerged when assessing a single widely distributed PFT (broadleaved trees; Fig. 5c). Thus, in addition to area-based rates of R_{dark}^{25} at any given photosynthetic capacity being fastest in C$_3$ herbs, $R_{dark,a}^{25}$ was also faster in plants growing in cold environments.

Analyzed on a mass basis, tests for common slopes among $R_{dark,m}^{25} \leftrightarrow V_{cmax,m}^{25}$ relationships revealed significant differences among PFTs and TWQ classes. Among PFTs, the slope of the $R_{dark,m}^{25} \leftrightarrow V_{cmax,m}^{25}$ relationship was greatest in C$_3$ herbs/grasses and smallest in needle-leaved trees (Fig. 5d; Table S3); thus, variation in mass-based photosynthetic capacity was matched by greater variation in leaf $R_{dark,m}^{25}$ in herbs/grasses than in needled-leaved trees. Although the effect of TWQ on $R_{dark,m}^{25} \leftrightarrow V_{cmax,m}^{25}$ was not as consistent as for area-based relationships, in general the pattern was for $R_{dark,m}^{25}$ at any given $V_{cmax,m}^{25}$ to be fastest in plants growing in the coldest habitats, particularly when considering species that exhibit rapid metabolic rates (Fig. 5e,f).

Fig. 6 shows PFT- and TWQ-dependent variation in $R_{dark}^{25} \leftrightarrow [N]$. Assessed on a leaf-area basis, tests for common slopes revealed no significant differences among PFTs (Fig. 6a) or TWQ classes (Fig. 6b). The elevation of the relationships differed such that at any given leaf $[N]_a$, rates of $R_{dark,a}^{25}$ were ranked in order of C$_3$ herbs/grasses > shrubs > broadleaved trees = needle-leaved trees (Table S3). Considering all PFTs collectively, rates of $R_{dark,a}^{25}$ at any given $[N]_a$ were fastest in the coldest-grown
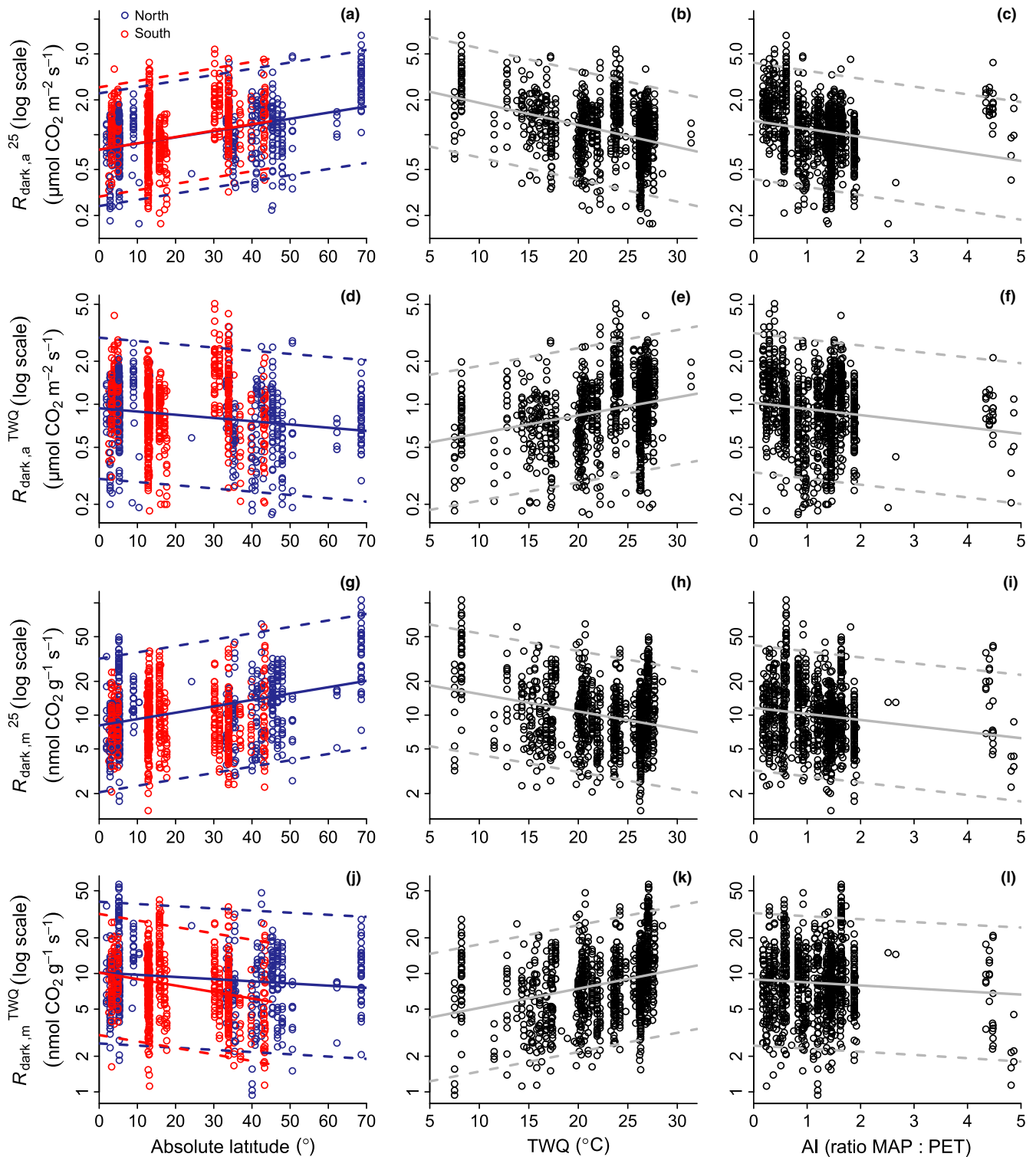
Fig. 4 Relationships between leaf dark respiration (R_{dark}; $\log_{10}$ scale) and location (absolute latitude) or climate (mean temperature of the warmest quarter (TWQ) and aridity index (AI)). (a–l) Traits shown are $R_{dark,a}^{25}$ (a–c) and $R_{dark,a}^{TWQ}$ (d–f), predicted area-based R_{dark} rates at 25°C and TWQ, respectively; $R_{dark,m}^{25}$ (g–i) and $R_{dark,m}^{TWQ}$ (j–l), predicted mass-based R_{dark} rates at 25°C and TWQ, respectively. Values shown are averages for unique site–species combinations for rates at 25°C and TWQ, calculated assuming a temperature-dependent Q_{10} (Tjoelker et al., 2001) and eqn 7 described in Atkin et al. (2005). Values at the TWQ of each replicate were calculated using climate/location data from the WorldClim database (Hijmans et al., 2005). AI is calculated as the ratio of mean annual precipitation (MAP) to mean annual potential evapotranspiration (PET) (UNEP, 1997). In plots against latitude, northern and southern latitudes are shown as blue and red symbols, respectively. Solid lines in each plot are regression lines where the relationships were significant; dashed lines are the prediction intervals (two-times the SD) around the predicted relationship. See Table 3 for correlations between $\log_{10}$-transformed R_{dark} and location/climate. Note: see Fig. S3 for relationships between R_{dark} and AI, excluding data from the exceptionally high rainfall sites at Franz Josef on the South Island of New Zealand.

Table 3 Correlations between $\log_{10}$-transformed leaf respiration (R_{dark}) and location/climate (see Fig. 4)

Response variable	Hemisphere	Latitude							TWQ, both hemispheres							Aridity index, both hemispheres						
		df	P-value	r^2	Intercept	Slope	CI slope, lower	CI slope, higher	df	P-value	r^2	Intercept	Slope	CI slope, lower	CI slope, higher	df	P-value	r^2	Intercept	Slope	CI slope, lower	CI slope, higher
$\log R_{dark,a}^{25}$	North	404	<0.0001	0.189	-0.130	0.005	0.004	0.006	1104	<0.0001	0.139	0.467	-0.019	-0.022	-0.016	1069	<0.0001	0.038	0.119	-0.069	-0.090	-0.048
	South	698	<0.0001	0.071	-0.063	0.005	0.004	0.007														
$\log R_{dark,a}^{TWQ}$	North	404	<0.0001	0.039	-0.028	-0.002	-0.003	-0.001	1104	<0.0001	0.066	-0.329	0.013	0.010	0.015	1069	<0.0001	0.016	0.011	-0.043	-0.063	-0.023
	South	698	0.740	0.000	N/A	N/A	N/A	N/A														
$\log R_{dark,m}^{25}$	North	421	<0.0001	0.148	0.908	0.006	0.004	0.007	1111	<0.0001	0.074	1.342	-0.015	-0.019	-0.012	1076	<0.0001	0.019	1.065	-0.054	-0.077	-0.031
	South	688	0.824	0.000	N/A	N/A	N/A	N/A														
$\log R_{dark,m}^{TWQ}$	North	421	0.006	0.018	1.008	-0.002	-0.003	-0.001	1111	<0.0001	0.083	0.546	0.016	0.013	0.019	1076	0.031	0.004	0.950	-0.026	-0.049	-0.002
	South	688	<0.0001	0.061	0.991	-0.005	-0.007	-0.004														

For each correlation between the y-axis leaf trait and x-axis location/climate parameter, the number of degrees of freedom (df), probability value (P-value) and coefficient of determination (r^2) and 95% confidence intervals (CI) are shown. Traits shown are: $R_{dark,a}^{25}$ and $R_{dark,a}^{TWQ}$, predicted area-based leaf R_{dark} rates (μmol CO_2 m^{-2} s^{-1}) at 25°C and mean temperature of the warmest quarter (TWQ), respectively; leaf $R_{dark,m}^{25}$ and $R_{dark,m}^{TWQ}$, predicted mass-based R_{dark} rates (nmol CO_2 g^{-1} s^{-1}) at 25°C and TWQ, respectively. TWQ at each site were obtained using site information and the WorldClim database (Hijmans et al., 2005). Aridity index is calculated as the ratio of mean annual precipitation (MAP) to mean annual potential evapotranspiration (PET) (UNEP, 1997; Zomer et al., 2008). N/A, not applicable.

plants, with the overall pattern being one of decreasing $R_{dark,a}^{25}$ with increasing TWQ (Fig. 6b). Within broadleaved trees, slopes of $R_{dark,a}^{25} \leftrightarrow [N]_a$ relationships differed significantly, being greater at sites with TWQ values of 15–20°C compared with the two remaining warmer TWQ categories (Table S3). Hence, for broadleaved tree species with high $[N]_a$, $R_{dark,a}^{25}$ was faster in cold habitats than in their warmer counterparts, at least when considering TWQ classes > 15°C. Analyzing $R_{dark}^{25} \leftrightarrow [N]$ on a mass basis revealed significant slope differences among PFTs (Fig. 6d) and TWQ classes (Fig. 6e,f). For the latter, the overall pattern was one of increasing $R_{dark,m}^{25} \leftrightarrow [N]_m$ slope in plants growing at the colder sites.

Mixed-effects model analyses

Fitting linear mixed-effects models confirmed that the assigned JULES PFTs accounted (in conjunction with assigned random effects) for much of the variation in area-based R_{dark}^{25} present in the GlobResp database. For example, a 'null' model where fixed effects were limited to four PFT classes (with species, families, and sites treated as random effects) explained 48% of variation in the $R_{dark,a}^{25}$ response (i.e. $r^2 = 0.48$; Table 5a); for an equivalent model that did not include any random effects, inclusion of the four PFT classes alone as fixed terms explained 27% of the variation in $R_{dark,a}^{25}$. Inclusion of additional fixed terms resulted in an increase in the explanatory power of the 'best' predictive model, such that 70% of variation in $R_{dark,a}^{25}$ was accounted for via inclusion of $[N]_a$, $[P]_a$, $V_{cmax,a}^{25}$ and TWQ (Figs 7a, S3–S5). The variance components of the preferred model, as defined by the random term (Table 5), indicated that while species and family (Fig. S6) only accounted for c. 8% of the unexplained variance (i.e. the response variance not accounted for by the fixed terms), c. 23% was related to site differences (Fig. S7; Table 5a). Importantly, the linear mixed-effects model confirmed that $R_{dark,a}^{25}$ decreased with increasing growth T (TWQ; Table 5). Using mass-based variables, the assigned PFTs again accounted for much of the variation in $R_{dark,m}^{25}$ in the GlobResp database (Table 5), with the 'null' model explaining 54% of variation in $R_{dark,m}^{25}$. Inclusion of additional leaf-trait (but not climate) fixed terms resulted in 78% of variation in $R_{dark,m}^{25}$ being accounted for (Fig. 7b). For both the area- and mass-based mixed-effect models, the 'best' predictive model (as assessed by AIC; Table S4) yielded predictive PFT-specific equations (Table 6). Table S5 provides a comparison of models using alternative PFT classifications (JULES and LPJ); these analyses revealed that replacing JULES PFTs with those of LPJ did not improve the power of the predictive models, as shown by the lower AIC values for a model that used JULES PFTs than for one using LPJ PFTs (Table S5).

Discussion

Recognizing that leaf respiration is not adequately represented in terrestrial biome models and the land surface component of ESMs (Leuzinger & Thomas, 2011; Huntingford et al., 2013) – reflecting the previous lack of data to constrain estimates of leaf R_{dark} – and that improving predictions of future vegetation–climate

Table 4 Regression equations expressing area- and mass-based leaf dark respiration at 25°C ($R_{dark}{}^{25}$) as a function of other leaf traits and site climate

Dependent variable	Input: independent variables (Backwards-stepwise regression)	Output: selected equations (Multiple linear regression)	Multiple linear regression parameters			Standardized partial regression coefficients				
			n	r^2	PRESS statistic	β_1	β_2	β_3	β_4	β_5
Area-based $\log_{10} R_{dark,a}{}^{25}$	Leaf traits (all $\log_{10}$): $[N]_a$, M_a	$\mathrm{Log_{10}}R_{dark,a}{}^{25} = -0.469 + (0.329 \times \log_{10}N_a) + (0.204 \times \log_{10} M_a)$	1038	0.168	57.71	0.270 ($\log_{10}N_a$)	0.186 ($\log_{10} M_a$)			
	Leaf traits (all $\log_{10}$): $[N]_a$, $[P]_a$, M_a	$\mathrm{Log_{10}}R_{dark,a}{}^{25} = 0.076 + (0.304 \times \log_{10} P_a) + (0.140 \times \log_{10} M_a)$	730	0.156	40.95	0.338 ($\log_{10} P_a$)	0.112 ($\log_{10} M_a$)			
	Leaf traits (all $\log_{10}$): $[N]_a$, $[P]_a$, M_a, $V_{cmax,a}{}^{25}$	$\mathrm{Log_{10}}R_{dark,a}{}^{25} = -0.241 + (0.235 \times \log_{10} P_a) + (0.050 \times \log_{10} M_a) + (0.290 \times \log_{10} V_{cmax,a}{}^{25})$	703	0.221	34.79	0.269 ($\log_{10} P_a$)	0.041 ($\log_{10} M_a$)	0.285 ($\log_{10} V_{cmax,}$)		
	Climate parameters: TWQ, PWQ, AI	$\mathrm{Log_{10}}R_{dark,a}{}^{25} = 0.451 - (0.0153 \times TWQ) - (0.00016 \times PWQ)$	1114	0.171	61.86	−0.297 (TWQ)	−0.196 (PWQ)			
	Leaf traits (all $\log_{10}$) and climate parameters: $[N]_a$, $[P]_a$, M_a, $V_{cmax,a}{}^{25}$, TWQ, PWQ	$\mathrm{Log_{10}}R_{dark,a}{}^{25} = -0.563 + (0.292 \times \log_{10} M_a) + (0.119 \times \log_{10} P_a) + (0.221 \times V_{cmax,a}{}^{25}) - (0.0147 \times TWQ) - (0.00012 \times PWQ)$	703	0.353	29.06	0.238 ($\log_{10} M_a$)	0.136 ($\log_{10} P_a$)	0.243 ($\log_{10} V_{cmax,}$)	−0.304 (TWQ)	−0.165 (PWQ)
Mass-based $\log_{10} R_{dark,m}{}^{25}$	Leaf traits (all $\log_{10}$): $[N]_m$, SLA	$\mathrm{Log_{10}}R_{dark,m}{}^{25} = 0.0932 + (0.475 \times \log_{10}SLA) + (0.364 \times \log_{10}N_m)$	1037	0.314	57.78	0.392 ($\log_{10}SLA$)	0.244 ($\log_{10}N_m$)			
	Leaf traits (all $\log_{10}$): $[N]_m$, $[P]_m$, SLA	$\mathrm{Log_{10}}R_{dark,m}{}^{25} = 0.495 + (0.556 \times \log_{10}SLA) + (0.333 \times \log_{10}P_m)$	730	0.336	40.68	0.396 ($\log_{10}SLA$)	0.315 ($\log_{10}P_m$)			
	Leaf traits (all $\log_{10}$): $[N]_m$, $[P]_m$, SLA, $V_{cmax,m}{}^{25}$	$\mathrm{Log_{10}}R_{dark,m}{}^{25} = -0.061 + (0.432 \times \log_{10}SLA) + (0.264 \times \log_{10}P_m) + (0.274 \times \log_{10} V_{cmax,m}{}^{25})$	703	0.407	34.80	0.307 ($\log_{10}SLA$)	0.252 ($\log_{10}P_m$)	0.263 ($\log_{10} V_{cmax,}$)		
	Climate parameters: TWQ, PWQ, AI	$\mathrm{Log_{1}0}R_{dark,m}{}^{25} = 1.353 - (0.0157 \times TWQ) - (0.000018*AI)$	1121	0.087	83.22	−0.276 (TWQ)	0.112 (AI)			
	Leaf traits (all $\log_{10}$) and climate parameters: $[N]_m$, $[P]_m$, SLA, $V_{cmax,m}{}^{25}$, TWQ, AI	$\mathrm{Log_{10}}R_{dark,m}{}^{25} = 0.249 + (0.526 \times \log_{10}SLA) + (0.0705 \times \log_{10}P_m) + (0.281 \times \log_{10}V_{cmax,m}{}^{25}) - (0.0184 \times TWQ) - (0.000015 \times AI)$	703	0.497	29.72	0.374 ($\log_{10}SLA$)	0.067 ($\log_{10}P_m$)	0.270 ($\log_{10}V_{cmax,}$)	−0.333 (TWQ)	0.111 (AI)

All leaf trait data were $\log_{10}$-transformed. To select the best-fitting equation from a group of input independent variables (e.g. leaf trait, climate, or the combination of trait plus climate), data were explored using backwards-stepwise regression – this revealed that chosen parameters exhibited variance inflation factors (VIFs) < 2.0 (i.e. minimal multicollinearity); it also identified best-fitting parameters (using F-to-remove criterion). Thereafter, multiple regression analyses were conducted to estimate predictive equations for the chosen variables. All selected variables were significant ($P < 0.001$). The PRESS statistic (predicted residual error sum of squares) provides a measure of how well each regression model predicts the observations, with smaller PRESS indicating better predictive capability. Relative contributions of leaf trait and climate variables to each regression can be gauged from their standardized partial regression coefficients ($\beta_1–\beta_5$, depending on model equation). M_a, leaf mass per unit leaf area (g m^{-2}); SLA, leaf area per unit leaf mass (m^2 kg^{-1}); $[N]_a$ and $[N]_m$, area- (g m^{-2}) and mass-based (mg g^{-1}) leaf nitrogen concentration, respectively; $[P]_a$ and $[P]_m$, area- (g m^{-2}) and mass-based (mg g^{-1}) leaf phosphorus concentration, respectively; $V_{cmax,a}{}^{25}$ (μmol CO$_2$ m^{-2} s^{-1}) and $V_{cmax,m}{}^{25}$ (nmol CO$_2$ g^{-1} s^{-1}), predicted area- and mass-based capacity for CO$_2$ fixation by Rubisco at 25°C, respectively; $R_{dark,a}{}^{25}$ (μmol CO$_2$ m^{-2} s^{-1}) and $R_{dark,m}{}^{25}$ (nmol CO$_2$ g^{-1} s^{-1}), predicted area- and mass-based leaf R_{dark} rates at 25°C, respectively; TWQ, mean temperature of the warmest quarter (i.e. warmest 3-month period yr^{-1}; °C); MAP, mean annual precipitation (mm yr^{-1}); PWQ, mean precipitation of the warmest quarter; AI, aridity index, calculated as the ratio of MAP to mean annual potential evapotranspiration (UNEP, 1997; Zomer et al., 2008). TWQ at each site was obtained using site information and the WorldClim database (Hijmans et al., 2005).
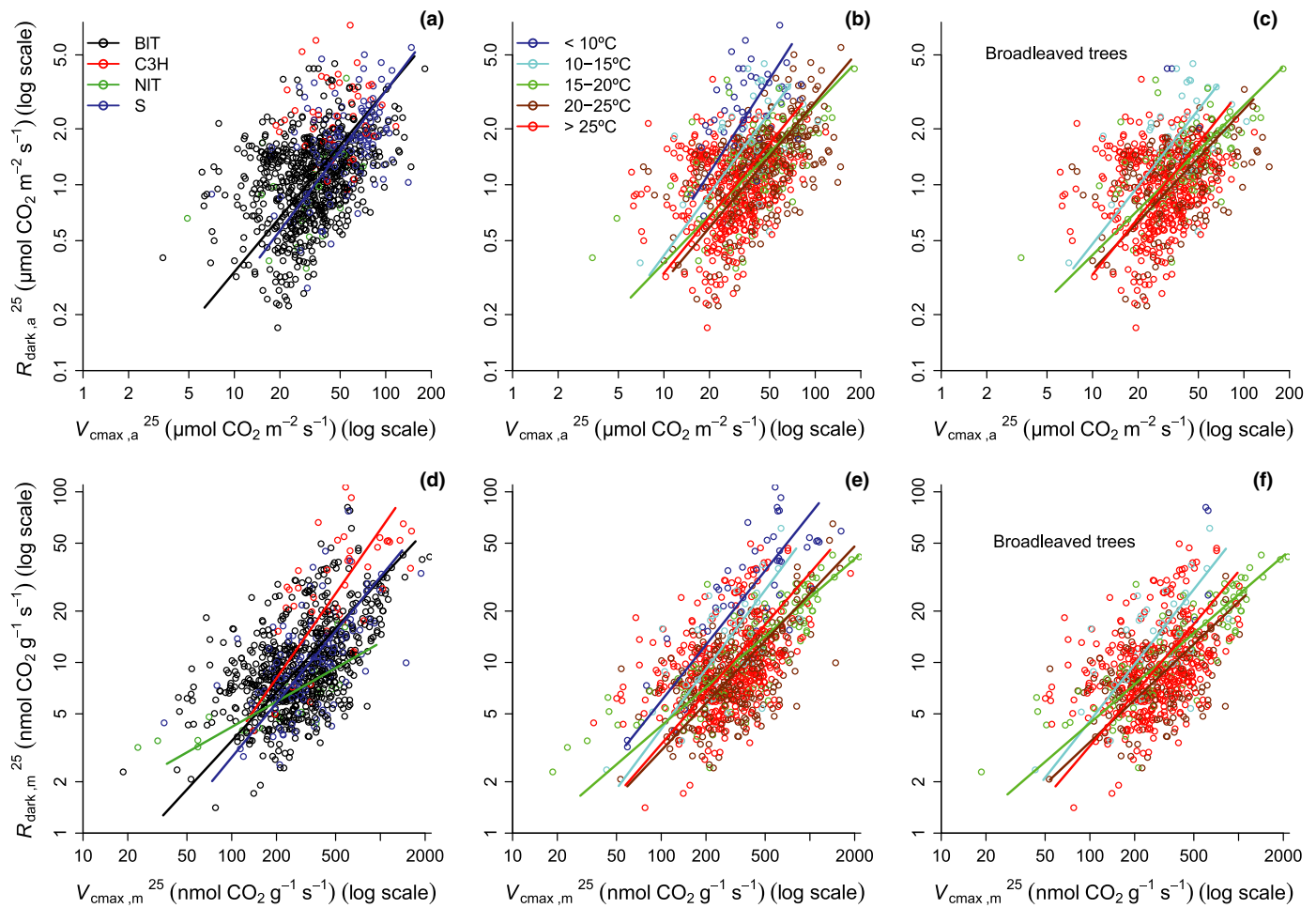
Fig. 5 Patterning of area- and mass-based R_{dark}^{25}–V_{cmax}^{25} relationships by Joint UK Land Environment Simulator (JULES) plant functional types (PFTs; a, d); mean temperature of the warmest quarter (TWQ) categories (5°C intervals) – all data (b, e); and TWQ categories (5°C intervals) – broadleaved trees only (c, f). All values shown on a log_{10} scale. Values shown are averages for unique site–species combinations. Upper panels (a–c) show area-based values, while lower panels (d–f) show mass-based values. JULES PFTs: BlT, broadleaved tree; C3H, C$_3$ metabolism herb/grass; NlT, needle-leaved tree; S, shrub. TWQ classes: 1st, < 10°C; 2nd, 10–15°C; 3rd, 15–20°C; 4th, 20–25°C; 5th, > 25°C. Values of leaf dark respiration (R_{dark}) at 25°C were calculated assuming a T-dependent Q_{10} (Tjoelker *et al.*, 2001) and eqn 7 described in Atkin *et al.* (2005). Values of V_{cmax} at 25°C were calculated according to Farquhar *et al.* (1980) assuming an activation energy (E_a) of 64.8 kJ mol^{-1}. See Table S3 for standardized major axis (SMA) regression outputs.

scenarios requires global variation in leaf R_{dark} to be more thoroughly characterized (Atkin *et al.*, 2014), we compiled and analyzed a new, large global database of leaf R_{dark}, climate conditions and associated traits. Our findings revealed systematic variation in leaf R_{dark} in contrasting environments, particularly with regard to site-to-site differences in growth T and, to a lesser extent, aridity. Importantly, analysis of the GlobResp database has yielded a range of equations (suitable for TBMs and land surface components of ESMs) to predict variations in R_{dark} using information on associated traits (particularly photosynthetic capacity, as well as leaf structure and chemistry) and growth T at each site.

Global patterns in leaf respiration: role of environmental gradients

Our results suggest, irrespective of whether rates are expressed on an area or mass basis, that the global pattern is one of increasing rates of leaf R_{dark} with site growth T (Figs 4, S4) when moving

from the cold, dry Arctic tundra to the warm, moist tropics. Importantly, however, such increases in leaf R_{dark} are far less than expected given the large range of growth T across sites. One would expect the variation in TWQ across our sites (*c.* 20°C) to be associated with an approximate fourfold increase in R_{dark}^{TWQ} (assuming that R_{dark} roughly doubles for every instantaneous 10°C rise in T) rather than the observed approximate twofold increases (Fig. 4). Underpinning this constrained variation in R_{dark}^{TWQ} are markedly faster area- and mass-based rates of leaf R_{dark} at 25°C (R_{dark}^{25}) at the coldest sites, and slower R_{dark}^{25} at warmer sites near the equator (Figs 4, S4).

Earlier studies of temperature responses were contradictory: some report faster area- and/or mass-based rates of R_{dark}^{25} at cold sites (Stocker, 1935; Wager, 1941; Semikhatova *et al.*, 1992, 2007), whilst others have found similar mass-based rates of R_{dark}^{25} and $R_{dark,m}^{25}$↔[N]$_m$ relationships in (woody) plants growing in cold and warm habitats (Reich *et al.*, 1998a; Wright *et al.*, 2006). Our new global database, which includes data from
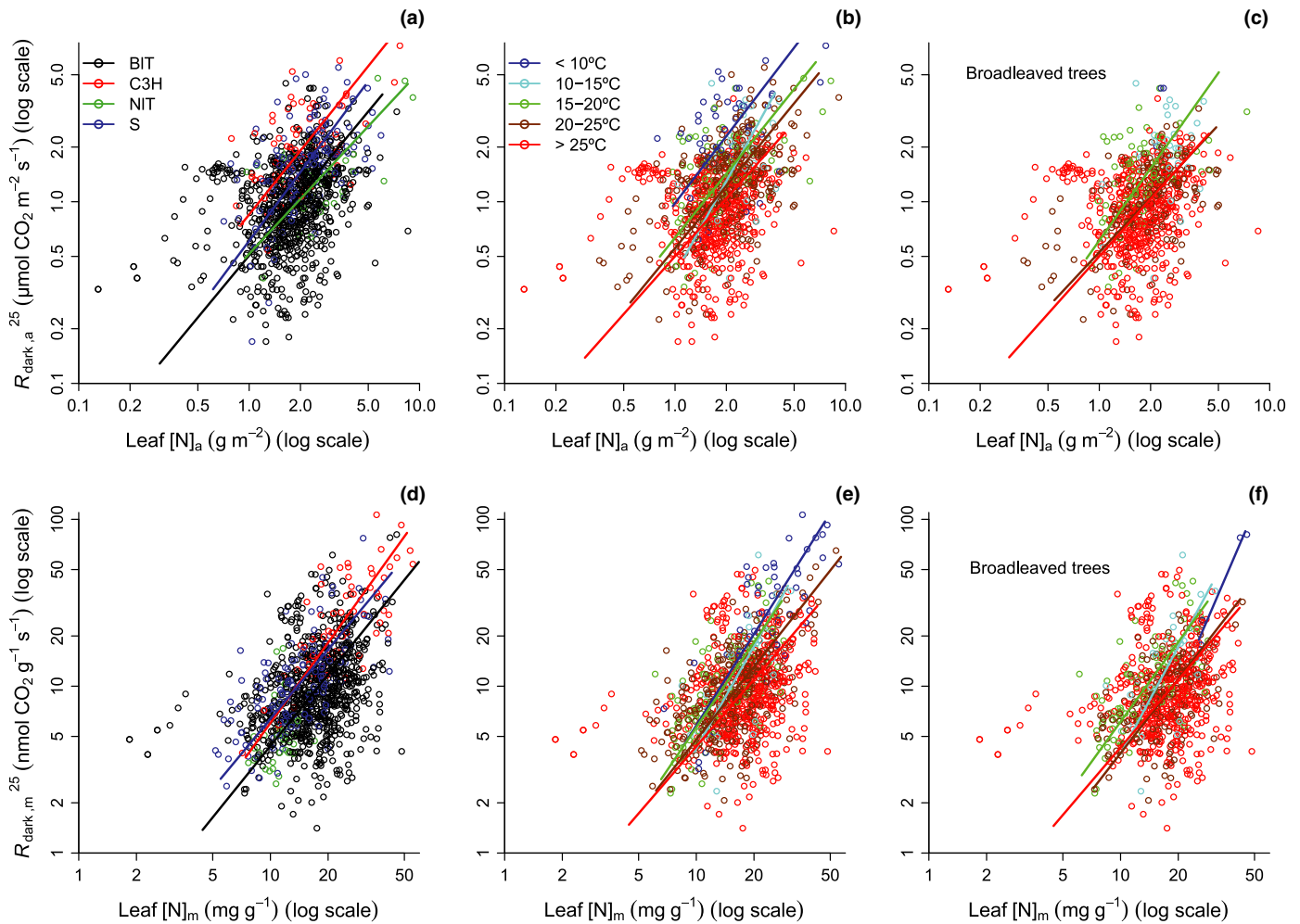
Fig. 6 Patterning of area- and mass-based R_{dark}^{25}–nitrogen (N) relationships by Joint UK Land Environment Simulator (JULES) plant functional types (PFTs; a, d); mean temperature of the warmest quarter (TWQ) categories (5°C intervals) – all data (b, e); and TWQ categories (5°C intervals) – broadleaved trees only (c, f). Values shown are averages for unique site–species combinations. All values shown on a $\log_{10}$ scale. JULES PFTs: BlT, broadleaved tree; C3H, C_3 metabolism herb/grass; NlT, needle-leaved tree; S, shrub. TWQ classes: 1st, < 10°C; 2nd, 10–15°C; 3rd, 15–20°C; 4th, 20–25°C; 5th, > 25°C. Values of leaf dark respiration (R_{dark}) at 25°C were calculated assuming a T-dependent Q_{10} (Tjoelker et al., 2001) and eqn 7 described in Atkin et al. (2005). See Table S3 for standardized major axis (SMA) regression outputs.

Reich et al. (1998a) and Wright et al. (2006), contains numerous, previously unpublished data for tropical forest and Arctic tundra sites (Tables 1, S1), greatly expanding the thermal range and species coverage. Whilst one might argue that the faster area- and mass-based R_{dark}^{25} in cold habitats (Figs 4, S4) is a result of the inclusion of tundra herbs/grasses in the GlobResp database, growth T (i.e. TWQ) remained important when analyzing $R_{dark}^{25} \leftrightarrow V_{cmax}^{25}$ and $R_{dark}^{25} \leftrightarrow [N]$ relationships within a single, globally distributed PFT (broadleaved trees; Figs 5c, 6c). Moreover, the significant negative $R_{dark,a}^{25} \leftrightarrow TWQ$ and $R_{dark,m}^{25} \leftrightarrow TWQ$ relationships (Fig. 4) were maintained when data were restricted to broadleaved trees (data not shown), albeit with a diminished slope for $R_{dark,m}^{25} \leftrightarrow TWQ$ relationships. So, when analyzed at the global level, our key finding is that rates of R_{dark}^{25} do differ between cold and warm sites.

Faster R_{dark}^{25} in plants growing in cold habitats than in those in warm habitats could reflect phenotypic (acclimation) or genotypic differences across gradients in growth T. The ability of leaf

R_{dark} to acclimate to sustained changes in growth T appears widespread among different PFTs (Atkin & Tjoelker, 2003; Campbell et al., 2007), although there is some evidence that broadleaved trees may have a greater capacity to acclimate than their conifer counterparts (Tjoelker et al., 1999). Acclimation to low growth T is linked to reversible adjustments in respiratory metabolism (Atkin & Tjoelker, 2003). Rapid leaf R_{dark} is inherent in a number of species characteristic of cold habitats (Larigauderie & Körner, 1995; Xiang et al., 2013). Similarly, there is evidence that within species, genotypes from cold habitats can exhibit inherently faster leaf R_{dark} than genotypes from warmer habitats (Mooney, 1963; Oleksyn et al., 1998). However, the pattern (both among and within species) is far from consistent (Chapin & Oechel, 1983; Atkin & Day, 1990; Collier, 1996).

Another site factor that might influence R_{dark}^{25} is water availability or aridity (Figs 4, S3; Tables 4, 5). In our study, faster leaf R_{dark}^{25} occurred at the driest sites; similar findings were reported by Wright et al. (2006). Although literature reviews suggest that

New
Phytologist

Table 5 Two linear mixed-effects models ('best' predictive model and a 'null', plant functional type (PFT) only model), with area-based (μmol CO_2 m^{-2} s^{-1}) (a) and mass-based (nmol CO_2 g^{-1} s^{-1}) (b) leaf respiration at 25°C ($R_{dark,a}^{25}$ and $R_{dark,m}^{25}$, respectively) as the response variables, each showing fixed and random effects

Fixed effects

Source	'Best' predictive model (PFTs, leaf traits and climate)			'Null' model (PFT only)		
	Value	SE	t-value	Value	SE	t-value
(a) Area-based model						
PFT-BlT	1.2636	0.033	38.551	1.3805	0.046	29.750
PFT-C3H	0.4708	0.141	3.348	0.5099	0.160	3.185
PFT-NIT	−0.3595	0.150	−2.392	−0.0558	0.179	−0.311
PFT-S	0.3290	0.064	5.163	0.3460	0.071	4.867
[N]$_a$	0.0728	0.018	4.124			
[P]$_a$	0.0015	0.000	7.389			
$V_{cmax,a}^{25}$	0.0095	0.001	15.241			
TWQ	−0.0358	0.006	−5.658			
Interaction: C3H × [N]$_a$	0.3394	0.069	4.892			
Interaction: NIT × [N]$_a$	0.0762	0.146	0.523			
Interaction: S × [N]$_a$	0.0687	0.053	1.295			
(b) Mass-based model						
PFT-BlT	8.5341	2.091	4.081	10.8938	1.243	8.764
PFT-C3H	−5.6273	6.832	−0.824	10.0926	3.569	2.828
PFT-NIT	6.8086	16.683	0.408	−2.2741	3.553	−0.640
PFT-S	−2.9249	2.564	−1.141	1.8429	1.492	1.235
[N]$_m$	−0.1306	0.085	−1.531			
[P]$_m$	−0.5670	1.491	−0.380			
M_a	−0.0137	0.004	−3.040			
$V_{cmax,m}^{25}$	0.0111	0.002	6.459			
Interaction: C3H × [N]$_m$	0.7252	0.295	2.459			
Interaction: NIT × [N]$_m$	−0.7283	1.796	−0.405			
Interaction: S × [N]$_m$	0.1605	0.146	1.102			
Interaction: C3H × [P]$_m$	−4.2308	2.659	−1.591			
Interaction: NIT × [P]$_m$	0.4131	1.694	0.244			
Interaction: S × [P]$_m$	2.3333	1.790	1.303			
Interaction: [N]$_m$ × [P]$_m$	0.1876	0.062	3.026			

Random effects

Source	'Best' predictive model (PFTs, leaf traits and climate)			'Null' model (PFT only)	
	No. of levels per group	Residual variance	% of total	Residual variance	% of total
(a) Area-based model					
Intercept variance: species	531	0.009	7.1	0.023	11.5
Intercept variance: families	100	0.002	1.4	0.004	2.1
Intercept variance: sites	49	0.031	23.4	0.073	36.2
Residual error		0.091	68.2	0.102	50.2
Total		0.133	100.0	0.202	100.0
(b) Mass-based model					
Intercept variance: families	100	0.373	0.7	7.950	9.2
Intercept variance: sites	49	37.745	73.2	55.290	64.2
Residual error		13.476	26.1	22.850	26.5
Total		51.594	100.0	86.090	100.0

See Table 6 for PFT-specific equations that can be used to predict variability in $R_{dark,a}^{25}$ and $R_{dark,m}^{25}$ based on 'best' models. For the 'best' models, parameter values, SE and t-values are given for the continuous explanatory variables; explanatory variables (all untransformed and centered on their means) are: 1, plant functional types (PFT), according to Joint UK Land Environment Simulator (JULES; Clark et al., 2011): BlT (broadleaved tree), C3H (C3 metabolism herbs/grasses), NIT (needle-leaved trees), and S (shrubs); 2, leaf nitrogen ([N]) and phosphorus ([P]) concentrations (g m^{-2} for area-based values and mg g^{-1} for mass-based values), M_a (g m^{-2}) and Rubisco CO_2 fixation capacity at 25°C (V_{cmax}^{25}, μmol CO_2 m^{-2} s^{-1} and nmol CO_2 g^{-1} s^{-1} for area- and mass-based values, respectively); and mean temperature of the warmest quarter (TWQ, °C) (Hijmans et al., 2005). Fig. S5 assesses heterogeneity and normality assumptions of the 'best' models, while Fig. S6 shows model validation graphs for the area-based model fixed component explanatory variables; similarly, Fig. S7 shows details for variables omitted from the fixed components in the area-based model (M_a, AI and PWQ). The PFT-BlT values (first row) are based on the assumption that other variables were at their global mean values. For the random effects, the intercept was allowed to vary among species, families and sites; residual error represents variation within species, families and sites and measurement error. See Fig. 7 for scatter plots of modeled vs actual values of the 'best' models, both with and without inclusion of random effects. See also Table S4 for area-based model outputs for scenarios where different combinations of fixed-effects parameters were included.
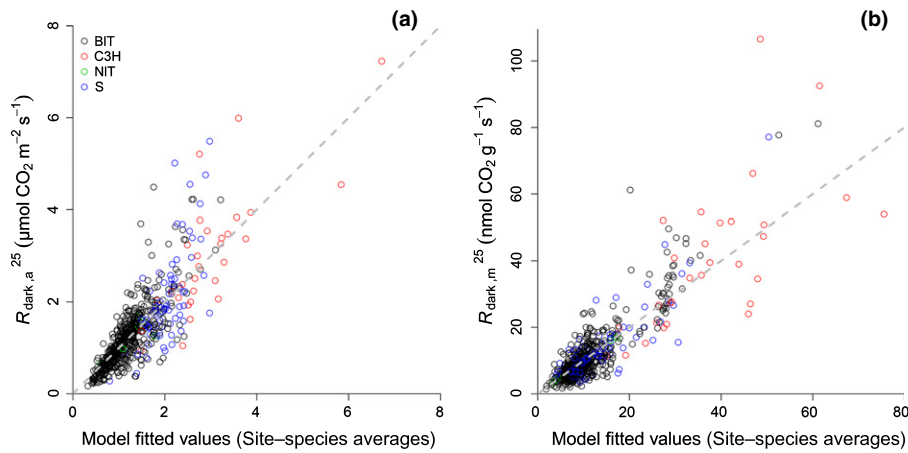
Fig. 7 Scatterplots for area-based (a) and mass-based (b) linear mixed-effects models' goodness of fits, including fixed and random terms. Observed values of leaf respiration at 25°C (R_{dark}^{25}) are plotted against model predictions (using the 'best' predictive models detailed in Table 5). (a) For the area-based model, the fixed component explanatory variables were: plant functional types (PFTs), according to Joint UK Land Environment Simulator (JULES; Clark *et al.*, 2011); area-based leaf nitrogen ($[N]_a$) and phosphorus ($[P]_a$) concentrations, and Rubisco CO_2 fixation capacity at 25°C ($V_{cmax,a}^{25}$); and mean temperature of the warmest quarter (TWQ) (Hijmans *et al.*, 2005). (b) For the mass-based model, the fixed component explanatory variables were: PFTs; mass-based leaf nitrogen ($[N]_m$) and phosphorus ($[P]_m$) concentrations, Rubisco CO_2 fixation capacity at 25°C ($V_{cmax,m}^{25}$), and leaf mass per unit leaf area (M_a).

Table 6 Plant functional type (PFT)-specific equations (formulated from the 'best' mixed-effects models shown in Table 5) that can be used to predict variability in area-based (μmol CO_2 m^{-2} s^{-1}) (a) and mass-based (nmol CO_2 g^{-1} s^{-1}) (b) leaf respiration at 25°C ($R_{dark,a}^{25}$ and $R_{dark,m}^{25}$, respectively)

(a) PFT-specific equations to predict variability in $R_{dark,a}^{25}$ ('best' model)

BlT: $R_{dark,a}^{25} = 1.2636 + (0.0728 \times [N]_a) + (0.015 \times [P]_a) + (0.0095 \times V_{cmax,a}^{25}) - (0.0358 \times TWQ)$

C3H: $R_{dark,a}^{25} = 1.7344 + (0.4122 \times [N]_a) + (0.015 \times [P]_a) + (0.0095 \times V_{cmax,a}^{25}) - (0.0358 \times TWQ)$

NlT: $R_{dark,a}^{25} = 0.9041 + (0.1489 \times [N]_a) + (0.015 \times [P]_a) + (0.0095 \times V_{cmax,a}^{25}) - (0.0358 \times TWQ)$

S: $R_{dark,a}^{25} = 1.5926 + (0.1415 \times [N]_a) + (0.015 \times [P]_a) + (0.0095 \times V_{cmax,a}^{25}) - (0.0358 \times TWQ)$

(b) PFT-specific equations to predict variability in $R_{dark,m}^{25}$ ('best' model)

BlT: $R_{dark,m}^{25} = 8.5341 - (0.1306 \times [N]_m) - (0.5670 \times [P]_m) - (0.0137 \times M_a) + (0.0111 \times V_{cmax,m}^{25}) + (0.1876 \times ([N]_m \times [P]_m))$

C3H: $R_{dark,m}^{25} = 2.9068 + (0.5946 \times [N]_m) - (4.7978 \times [P]_m) - (0.0137 \times M_a) + (0.0111 \times V_{cmax,m}^{25}) + (0.1876 \times ([N]_m \times [P]_m))$

NlT: $R_{dark,m}^{25} = 15.3427 - (0.8589 \times [N]_m) - (0.1539 \times [P]_m) - (0.0137 \times M_a) + (0.0111 \times V_{cmax,m}^{25}) + (0.1876 \times ([N]_m \times [P]_m))$

S: $R_{dark,m}^{25} = 5.6092 + (0.0299 \times [N]_m) + (1.7663 \times [P]_m) - (0.0137 \times M_a) + (0.0111 \times V_{cmax,m}^{25}) + (0.1876 \times ([N]_m \times [P]_m))$

Explanatory variables are: PFTs, according to Joint UK Land Environment Simulator (JULES; Clark *et al.*, 2011): BlT (broadleaved tree), C3H (C$_3$ metabolism herbs/grasses), NlT (needle-leaved trees), and S (shrubs); leaf nitrogen ([N]) and phosphorus ([P]) concentrations (g m^{-2} for area-based values and mg g^{-1} for mass based values), leaf mass per unit area (M_a) and Rubisco CO_2 fixation capacity at 25°C (V_{cmax}^{25}; μmol CO_2 m^{-2} s^{-1} and nmol CO_2 g^{-1} s^{-1} for area- and mass-based values, respectively); and mean temperature of the warmest quarter (TWQ, °C) (Hijmans *et al.*, 2005). Note: equations refer to un-transformed values of each response and explanatory variable. See also Table S4 for area-based model equations for scenarios where different combinations of fixed effect parameters were included.

drought-mediated increases in leaf R_{dark} are rare (Flexas *et al.*, 2005; Atkin & Macherel, 2009), there are reports showing that drought can indeed increase leaf R_{dark} (Slot *et al.*, 2008; Metcalfe *et al.*, 2010), and taxa present at drier sites may also exhibit drought adaptations. However, given our reliance on calculated values of aridity that may not reflect water availability/loss at field-relevant scales, we suggest that further work is needed to confirm the extent to which R_{dark}^{25} varies in response to aridity gradients.

Relationships linking respiration to other leaf traits

Including V_{cmax}^{25} as an explanatory variable markedly improved predictions of R_{dark}^{25}, on both an area and a mass basis. V_{cmax}^{25} also accounted for a greater proportion of variation in R_{dark}^{25} than did leaf [N] or [P], highlighting the strong functional

interdependency between photosynthetic capacity and R_{dark}^{25}. Past studies have reported that variation in R_{dark} is tightly coupled to variation in photosynthesis (Reich *et al.*, 1998a; Loveys *et al.*, 2003; Whitehead *et al.*, 2004), underpinned by chloroplast–mitochondrion interdependence in the light and dark (Krömer, 1995; Noguchi & Yoshida, 2008), and energy costs associated with phloem loading (Bouma *et al.*, 1995). Thus, the simplifying assumption by JULES and other modeling frameworks (Schwalm *et al.*, 2010; Smith & Dukes, 2013) that $R_{dark,a}^{25}$ is proportional to $V_{cmax,a}^{25}$ (Cox *et al.*, 1998) is robustly supported by our global analysis. However, even though there was no significant $R_{dark,a}^{25} \leftrightarrow V_{cmax,a}^{25}$ relationship for C$_3$ herbs/grasses in Fig. 5(a), overall this PFT exhibited faster rates of $R_{dark,a}^{25}$ at a given $V_{cmax,a}^{25}$ than other PFTs (Fig. 5a), with average $R_{dark,a}^{25}:V_{cmax,a}^{25}$ ratios being 0.078 for C$_3$ herbs, 0.045 for shrubs, 0.033 for broadleaved trees and 0.038 for needle-leaved

trees. Moreover, area- or mass-based R_{dark}^{25} at any given V_{cmax}^{25} differed among thermally contrasting sites, being faster at colder sites (Fig. 5b,e; Table S3). Given these issues, it is crucial that in TBMs and ESMs that link $R_{dark,a}^{25}$ to $V_{cmax,a}^{25}$, account is taken of PFTs and the impact of site growth T on the balance between respiratory and photosynthetic metabolism.

Our documentation of new predictive $R_{dark,a}^{25} \leftrightarrow [N]_a$ relationships, to account for variation among PFTs and site growth T (Fig. 6) provides an opportunity to improve the next generation of ESMs. We found that leaf R_{dark}^{25} at any given leaf [N] was faster in C_3 forbs/grasses than in their shrub and tree counterparts (on both an area and a mass basis), supporting the findings of Reich *et al.* (2008). In C_3 herbs/grasses, faster rates of R_{dark}^{25} at any given leaf [N] probably reflect greater relative allocation of leaf N to metabolic processes than to structural or defensive roles (Evans, 1989; Takashima *et al.*, 2004; Harrison *et al.*, 2009), combined with high demands for respiratory products. In addition to PFT-dependent changes in $R_{dark}^{25} \leftrightarrow [N]$ relationships, we also found that rates of leaf R_{dark}^{25} at any given leaf [N] were faster in plants growing at colder sites. This finding held when all PFTs were considered together, and also within the single, widespread PFT of broadleaved trees. Faster leaf R_{dark}^{25} at a given [N] therefore appears to be a general trait associated with leaf development in cold habitats (Atkin *et al.*, 2008).

Variability in leaf respiration rates within individual ecosystems

A key feature of scatterplots, such as in Fig. 4 (which presents species means at each site), was the substantial variation in species mean values of R_{dark} at any given latitude, or TWQ, or indeed, within any given site (frequently five- to 10-fold). This is in line with the diversity often reported in other leaf functional traits (chemical, structural, and metabolic) within natural ecosystems (Wright *et al.*, 2004; Fyllas *et al.*, 2009; Asner *et al.*, 2014). Furthermore, the range of variation in species mean values of R_{dark} was far larger than the two-fold shift in mean R_{dark} observed along major geographic gradients. Our understanding of which of these factors account for the wide range of respiratory rates exhibited by coexisting species is still rather poor (Atkin *et al.*, 2014). At an ecological level, the wide range in R_{dark} could reflect differences among coexisting species (e.g. position along the 'leaf economic spectrum'; Wright *et al.*, 2004; position within the conceptual 'competitive–stress tolerator–ruderal (CSR)' space; Grime, 1977).

Formulating equations that predict global variability in leaf respiration

One of our objectives was to develop equations that accurately predict mean rates of leaf R_{dark}^{25} observed across the globe. Our final, parsimonious mixed-effects models accounted for 70% of the variation in area-based R_{dark}^{25} (Fig. 7a) and 78% of the variation in mass-based R_{dark}^{25} (Fig. 7b). Such models provide equations that enable R_{dark}^{25} to be predicted using inputs from fixed terms such as PFT, growth T and leaf physiology/chemistry.

Here, we discuss the fixed effects of the area- and mass-based models.

For the area-based model, PFT category was the most important explanatory factor (e.g. in a model with no random effects, the JULES PFT classification alone accounted for 27% of the variability in $R_{dark,a}^{25}$), followed by $V_{cmax,a}^{25}$, $[P]_a$, TWQ and $[N]_a$ (Table 5a). Moreover, a comparative model that included random components, and where fixed effects were limited to the PFT classes, was still able to explain 43% of the variation in $R_{dark,a}^{25}$, suggesting that while these PFTs represent a simplification of floristic complexity, they nevertheless help to account for much of the global variation in area-based R_{dark}^{25}.

Interestingly, introducing information on phenological habit (i.e. evergreen vs deciduous) and biome by replacing the JULES PFTs with those of LPJ did not improve the quality of the predictive model (Table S5). This may appear counterintuitive, but could have arisen because the additional information contained in the LPJ PFT classifications was already captured in the 'best' predictive model's explanatory variables (i.e. M_a, $[N]_a$, $[P]_a$, and TWQ) shown in Table 5.

The final 'best' predictive model retained $V_{cmax,a}^{25}$, providing further support for a coupling of photosynthetic and respiratory metabolism (Krömer, 1995; Hoefnagel *et al.*, 1998; Noguchi & Yoshida, 2008). In terms of leaf chemistry, inclusion of $[N]_a$ reflects the coupling of respiratory and N metabolism (Tcherkez *et al.*, 2005), and energy demands associated with protein turnover (Penning de Vries, 1975; Bouma *et al.*, 1994; Zagdanska, 1995). Moreover, as $[N]_a$ is important to $V_{cmax,a}^{25}$, inclusion of $V_{cmax,a}^{25}$ in the model may to some extent obscure the role of $[N]_a$ *per se*. The significant interaction of PFT and $[N]_a$ demonstrates (Table 5) that variation in leaf $[N]_a$ has greater proportional effects on $R_{dark,a}^{25}$ in some PFTs (e.g. C_3 herbs/grasses) than in others (e.g. broadleaved trees), for the reasons outlined earlier. Retention of $[P]_a$ in the preferred model suggests that latitudinal variation in foliar [P] (Fig. S2) plays an important role in facilitating faster rates of leaf $R_{dark,a}^{25}$ at the cold high-latitude sites (Figs 4, S4) whilst limiting rates at P-deficient sites in some regions of the tropics (Townsend *et al.*, 2007; Asner *et al.*, 2014). These findings are likely to have particular relevance for predictions of $R_{dark,a}^{25}$ in TBMs that include dynamic representation of N and P cycling (Thornton *et al.*, 2007; Zaehle *et al.*, 2014).

While PFT category remained an explanatory factor in the final model for mass-based R_{dark}^{25} (Table 5), $V_{cmax,m}^{25}$ emerged as the single most important factor accounting for variability in $R_{dark,m}^{25}$. Importantly, all climate variables were excluded from the model, including site growth T (TWQ). Does this mean that variation in $R_{dark,m}^{25}$ is unrelated to site growth T, as previously suggested (Wright *et al.*, 2006)? Not necessarily; variation in R_{dark}^{25} on both area and mass bases was tightly linked to variation in site growth T (TWQ, Fig. 5). The absence of TWQ in the mass-based mixed model probably arose from the influence of site growth T on leaf $[N]_m$, leaf $[P]_m$ and M_a; all three traits vary in response to differences in site growth T (Reich & Oleksyn, 2004; Wright *et al.*, 2004; Poorter *et al.*, 2009).

In the preferred models for area- and mass-based R_{dark}^{25}, little of the response variance not accounted for by the fixed terms was

related to phylogeny, as represented by 'family' (Fig. S8); by contrast, a substantial component (23–73%) of the response variance not accounted for by the fixed terms was related to differences among sites (Fig. S9). This suggests that other 'site' factors (including environmental and methodological differences) may have played an important role in determining variation in $R_{dark, a}{}^{25}$. Soil characteristics may be important, including availability of nutrients such as calcium, potassium and magnesium (Broadley *et al.*, 2004). In addition, rates of $R_{dark}{}^{25}$ are sensitive to prevailing ambient T and soil water content in the days preceding measurement (Gorsuch *et al.*, 2010; Searle *et al.*, 2011). Given this, one would not expect long-term climate averages to fully capture the actual environment experienced by plants.

Looking forward: improving representation of leaf respiration in ESMs

The most direct way of improving representation of leaf respiration in TBMs and the land surface components of ESMs is to formulate equations that describe patterns in $R_{dark}{}^{25}$ using leaf trait and climate parameters already incorporated into those models. Our study provides PFT-, leaf trait- and climate-based equations, depending on which leaf traits are used in a particular model framework to predict variation in $R_{dark}{}^{25}$ (e.g. area- or mass-based [N], or photosynthetic capacity, Tables 5, S4, S5). Application of such equations would enable prediction of $R_{dark}{}^{25}$ for biogeographical regions for which the PFT composition is known. The GlobResp database will also assist in the development of land surface models that use a trait-continuum approach, where bivariate trait associations and tradeoffs are included directly in the models, rather than a strictly PFT-categorical approach. For an overview of the issues relevant to incorporation of trait–climate relationships in TBMs, readers are directed to recent discussion papers (Scheiter *et al.*, 2013; Verheijen *et al.*, 2013; Higgins *et al.*, 2014).

Other challenges to incorporating leaf respiration in ESMs include: establishing models of diel variations in leaf R_{dark} (here, understanding the extent to which our daytime measurements of R_{dark} differ from fluxes measured at night will be of interest); accounting for the appropriate degree of thermal acclimation of leaf $R_{dark}{}^{25}$ to dynamic changes in prevailing growth T and soil moisture at all geographical positions; and identifying the extent to which light inhibition of leaf respiration (Kok, 1948; Brooks & Farquhar, 1985; Hurry *et al.*, 2005) varies among PFTs and biomes, over the range of leaf Ts experienced by leaves during the day. Although much progress has been made (King *et al.*, 2006; Atkin *et al.*, 2008; Smith & Dukes, 2013; Wythers *et al.*, 2013), accounting for temperature acclimation and light inhibition of leaf R in TBMs and associated land surface components of ESMs remains a considerable challenge (Atkin *et al.*, 2014). The equations we provide here that predict current biogeographical variations in leaf R_{dark} at a standard T (typically 25°C) are driven by some unquantified combination of acclimation responses and genotypic (adaptive) differences. Further work is needed, however, to establish criteria that will enable environment and genotypic variations in light inhibition of leaf respiration to be

predicted; here, recent studies linking light inhibition to photorespiratory metabolism (Griffin & Turnbull, 2013; Ayub *et al.*, 2014) may provide directions for future research. Achieving these goals will be assisted by compilation of data not only from the sites shown in Fig. 1, but also from geographic regions currently poorly represented; additional data from Africa, Asia and Europe are needed to enable global historical biogeographic/phylogenetic effects on leaf R_{dark} to be tested. In the long term, a wider goal is development of a mechanistic model that accounts for genotypic–developmental–environmentally mediated variations in leaf R_{dark}.

Currently, many TBM and ESMs predict photosynthetic capacity ($V_{cmax}{}^{25}$) and $R_{dark}{}^{25}$ based on assumed [N] values for each PFT. In using this approach, differences among plants within a PFT (e.g. genotypic differences and/or plasticity responses to the growth environment) are unspecified. Our mixed-effects models suggest that PFTs capture a substantial amount of species variation across diverse sites and their use is reasonable as a first approximation for the purposes of modeling. In the application of PFT-based modeling, the growth T-dependent (TWQ) variations in $R_{dark}{}^{25}$ within widely distributed PFTs (e.g. broadleaved trees) provide a means to predict T adjustments in R_{dark} at the global scale. For example, predicted $R_{dark}{}^{25}$ declines 18% from 1.0 to 0.82 µmol m^{-2} s^{-1} when site temperature (TWQ) increases from 20 to 25°C (Table 6). Assuming a static PFT (e.g. no species turnover or differential acclimation/adaptation), these new equations (Table 6, and associated ESM equations in Table S4) provide a first-order approximation of the acclimation response of $R_{dark}{}^{25}$ of a given PFT to a cooler past world, or warmer future world. They also demonstrate that predictions based on PFT, leaf traits and TWQ provide a powerful improvement in the representation of leaf respiration in ESMs that seek to describe the role of terrestrial ecosystems in an evolving global climate and C cycle.

Acknowledgements

References

Allen SE. 1974. *Chemical analysis of ecological materials*. Oxford, UK: Blackwell Scientific Publications.

Amthor JS. 2000. The McCree-de Wit-Penning de Vries-Thornley respiration paradigms: 30 years later. *Annals of Botany* 86: 1–20.

Archibold OW. 1995. *Ecology of world vegetation*. London, UK: Chapman and Hall.

Asner GP, Martin RE, Tupayachi R, Anderson CB, Sinca F, Carranza-Jiménez L, Martinez P. 2014. Amazonian functional diversity from forest canopy chemical assembly. *Proceedings of the National Academy of Sciences, USA* 111: 5604–5609.

Atkin OK, Atkinson LJ, Fisher RA, Campbell CD, Zaragoza-Castells J, Pitchford J, Woodward FI, Hurry V. 2008. Using temperature-dependent changes in leaf scaling relationships to quantitatively account for thermal acclimation of respiration in a coupled global climate–vegetation model. *Global Change Biology* 14: 2709–2726.

Atkin OK, Bruhn D, Tjoelker MG. 2005. Response of plant respiration to changes in temperature: mechanisms and consequences of variations in Q_{10} values and acclimation. In: Lambers H, Ribas-Carbó M, eds. *Plant respiration: from cell to ecosystem*. Dordrecht, the Netherlands: Springer, 95–135.

Atkin OK, Day DA. 1990. A comparison of the respiratory processes and growth rates of selected Australian alpine and related lowland plant species. *Australian Journal of Plant Physiology* 17: 517–526.

Atkin OK, Evans JR, Siebke K. 1998. Relationship between the inhibition of leaf respiration by light and enhancement of leaf dark respiration following light treatment. *Australian Journal of Plant Physiology* 25: 437–443.

Atkin OK, Holly C, Ball MC. 2000. Acclimation of snow gum (*Eucalyptus pauciflora*) leaf respiration to seasonal and diurnal variations in temperature: the importance of changes in the capacity and temperature sensitivity of respiration. *Plant, Cell & Environment* 23: 15–26.

Atkin OK, Macherel D. 2009. The crucial role of plant mitochondria in orchestrating drought tolerance. *Annals of Botany* 103: 581–597.

Atkin OK, Meir P, Turnbull MH. 2014. Improving representation of leaf respiration in large-scale predictive climate–vegetation models. *New Phytologist* 202: 743–748.

Atkin OK, Scheurwater I, Pons TL. 2007. Respiration as a percentage of daily photosynthesis in whole plants is homeostatic at moderate, but not high, growth temperatures. *New Phytologist* 174: 367–380.

Atkin OK, Tjoelker MG. 2003. Thermal acclimation and the dynamic response of plant respiration to temperature. *Trends in Plant Science* 8: 343–351.

Atkin OK, Turnbull MH, Zaragoza-Castells J, Fyllas NM, Lloyd J, Meir P, Griffin KL. 2013. Light inhibition of leaf respiration as soil fertility declines along a post-glacial chronosequence in New Zealand: an analysis using the Kok method. *Plant and Soil* 367: 163–182.

Ayub G, Smith RA, Tissue DT, Atkin OK. 2011. Impacts of drought on leaf respiration in darkness and light in *Eucalyptus saligna* exposed to industrial-age atmospheric CO_2 and growth temperature. *New Phytologist* 190: 1003.

Ayub G, Zaragoza-Castells J, Griffin KL, Atkin OK. 2014. Leaf respiration in darkness and in the light under pre-industrial, current and elevated atmospheric CO_2 concentrations. *Plant Science* 226: 120–130.

Azcón-Bieto J, Lambers H, Day DA. 1983. Effect of photosynthesis and carbohydrate status on respiratory rates and the involvement of the alternative pathway in leaf respiration. *Plant Physiology* 72: 598–603.

Badger MR, Collatz GJ. 1977. Studies on the kinetic mechanism of ribulose-1,5-bisphosphate carboxylase and oxygenase reactions, with particular reference to the effect of temperature on kinetic parameters. *Carnegie Institution of Washington Yearbook* 76: 355–361.

Bartoli CG, Gomez F, Gergoff G, Guiamet JJ, Puntarulo S. 2005. Up-regulation of the mitochondrial alternative oxidase pathway enhances photosynthetic electron transport under drought conditions. *Journal of Experimental Botany* 56: 1269–1276.

Bolstad PV, Mitchell K, Vose JM. 1999. Foliar temperature–respiration response functions for broad-leaved tree species in the southern appalachians. *Tree Physiology* 19: 871–878.

Bolstad PV, Reich P, Lee T. 2003. Rapid temperature acclimation of leaf respiration rates in *Quercus alba* and *Quercus rubra*. *Tree Physiology* 23: 969–976.

Booth BBB, Jones CD, Collins M, Totterdell IJ, Cox PM, Sitch S, Huntingford C, Betts RA, Harris GR, Lloyd J. 2012. High sensitivity of future global warming to land carbon cycle processes. *Environmental Research Letters* 7: 024002.

Bouma TJ, De VR, Van LPH, De KMJ, Lambers H. 1995. The respiratory energy requirements involved in nocturnal carbohydrate export from starch-storing mature source leaves and their contribution to leaf dark respiration. *Journal of Experimental Botany* 46: 1185–1194.

Bouma TJ, Devisser R, Janssen JHJA, Dekock MJ, Vanleeuwen PH, Lambers H. 1994. Respiratory energy requirements and rate of protein turnover *in vivo* determined by the use of an inhibitor of protein synthesis and a probe to assess its effect. *Physiologia Plantarum* 92: 585–594.

Broadley MR, Bowen HC, Cotterill HL, Hammond JP, Meacham MC, Mead A, White PJ. 2004. Phylogenetic variation in the shoot mineral concentration of angiosperms. *Journal of Experimental Botany* 55: 321–336.

Brooks A, Farquhar GD. 1985. Effect of temperature on the CO_2/O_2 specificity of ribulose-1,5-biphosphate carboxylase/oxygenase and the rate of respiration in the light. Estimates from gas exchange measurements on spinach. *Planta* 165: 397–406.

von Caemmerer S, Evans JR, Hudson GS, Andrews TJ. 1994. The kinetics of ribulose-1,5-bisphosphate carboxylase/oxygenase *in vivo* inferred from measurements of photosynthesis in leaves of transgenic tobacco. *Planta* 195: 88–97.

Campbell C, Atkinson L, Zaragoza-Castells J, Lundmark M, Atkin O, Hurry V. 2007. Acclimation of photosynthesis and respiration is asynchronous in response to changes in temperature regardless of plant functional group. *New Phytologist* 176: 375–389.

Canadell JG, Le Quere C, Raupach MR, Field CB, Buitenhuis ET, Ciais P, Conway TJ, Gillett NP, Houghton RA, Marland G. 2007. Contributions to accelerating atmospheric CO_2 growth from economic activity, carbon intensity, and efficiency of natural sinks. *Proceedings of the National Academy of Sciences, USA* 104: 18866–18870.

Chapin FS, Oechel WC. 1983. Photosynthesis, respiration, and phosphate absorption by *Carex aquatilis* ecotypes along latitudinal and local environmental gradients. *Ecology* 64: 743–751.

Chazdon RL, Kaufmann S. 1993. Plasticity of leaf anatomy of two rainforest shrubs in relation to photosynethetic light acclimation. *Functional Ecology* 7: 385–394.

Clark DB, Mercado LM, Sitch S, Jones CD, Gedney N, Best MJ, Pryor M, Rooney GG, Essery RLH, Blyth E et al. 2011. The Joint UK Land Environment Simulator (JULES), model description – Part 2: carbon fluxes and vegetation dynamics. *Geoscientific Model Development* 4: 701–722.

Collier DE. 1996. No difference in leaf respiration rates among temperate, subarctic, and arctic species grown under controlled conditions. *Canadian Journal of Botany* 74: 317–320.

Cox PM, Betts RA, Jones CD, Spall SA, Totterdell IJ. 2000. Acceleration of global warming due to carbon-cycle feedbacks in a coupled climate model. *Nature* 408: 184–187.

Cox PM, Huntingford C, Harding RJ. 1998. A canopy conductance and photosynthesis model for use in a GCM land surface scheme. *Journal of Hydrology* 212: 79–94.

Craine JM, Berin DM, Reich PB, Tilman GD, Knops JMH. 1999. Measurement of leaf longevity of 14 species of grasses and forbs using a novel approach. *New Phytologist* 142: 475–481.

Crous KY, Zaragoza-Castells J, Löw M, Ellsworth DS, Tissue DT, Tjoelker MG, Barton CVM, Gimeno TE, Atkin OK. 2011. Seasonal acclimation of leaf respiration in *Eucalyptus saligna* trees: impacts of elevated atmospheric CO_2 and summer drought. *Global Change Biology* 17: 1560–1576.

Dillaway DN, Kruger EL. 2011. Leaf respiratory acclimation to climate: comparisons among boreal and temperate tree species along a latitudinal transect. *Tree Physiology* 31: 1114–1127.

Evans JR. 1989. Photosynthesis and nitrogen relationships in leaves of C_3 plants. *Oecologia* 78: 9–19.

Evans JR, Von Caemmerer S, Setchell BA, Hudson GS. 1994. The relationship between CO_2 transfer conductance and leaf anatomy in transgenic tobacco with a reduced content of Rubisco. *Australian Journal of Plant Physiology* 21: 475–495.

Falster DS, Warton DI, Wright IJ. 2006. *SMATR: standardised major axis tests and routines, version 2.0.* http://www.bio.mq.edu.au/ecology/SMATR/.

Farquhar GD, von Caemmerer S, Berry JA. 1980. A biochemical model of photosynthetic CO_2 assimilation in leaves of C_3 species. *Planta* 149: 78–90.

Fisher JB, Huntzinger DN, Schwalm CR, Sitch S. 2014. Modeling the terrestrial biosphere. *Annual Review of Environment and Resources* 39: 91–123.

Flexas J, Galmés J, Ribas-Carbó M, Medrano H, Lambers H. 2005. The effects of water stress on plant respiration. In: Lambers H, Ribas-Carbó M, eds. *Plant respiration: from cell to ecosystem, vol 18.* Dordrecht, the Netherlands: Springer, 85–94.

Fyllas NM, Patino S, Baker TR, Bielefeld Nardoto G, Martinelli LA, Quesada CA, Paiva R, Schwarz M, Horna V, Mercado LM et al. 2009. Basin-wide variations in foliar properties of Amazonian forest: phylogeny, soils and climate. *Biogeosciences* 6: 2677–2708.

García-Núñez C, Azócar A, Rada F. 1995. Photosynthetic acclimation to light in juveniles of two cloud-forest tree species. *Trees-Structure and Function* 10: 114–124.

Gifford RM. 2003. Plant respiration in productivity models: conceptualisation, representation and issues for global terrestrial carbon-cycle research. *Functional Plant Biology* 30: 171–186.

Gimeno TE, Sommerville KE, Valladares F, Atkin OK. 2010. Homeostasis of respiration under drought and its important consequences for foliar carbon balance in a drier climate: insights from two contrasting *Acacia* species. *Functional Plant Biology* 37: 323–333.

Gorsuch PA, Pandey S, Atkin OK. 2010. Temporal heterogeneity of cold acclimation phenotypes in *Arabidopsis* leaves. *Plant, Cell & Environment* 33: 244–258.

Griffin KL, Turnbull MH. 2013. Light saturated RuBP oxygenation by Rubisco is a robust predictor of light inhibition of respiration in *Triticum aestivum* L. *Plant Biol* 1: 1438–8677.

Grime JP. 1977. Evidence for the existence of three primary strategies in plants and its relevance to ecological and evolutionary theory. *The American Naturalist* 111: 1169–1194.

Grueters U. 1998. *Der Kohlenstoffhaushalt von Weizen in der Interaktion erhöhter CO_2/O_3 Konzentrationen und Stickstoffversorgung.* PhD thesis, Justus-Liebig-University Giessen, Giessen, Germany.

Harrison MT, Edwards EJ, Farquhar GD, Nicotra AB, Evans JR. 2009. Nitrogen in cell walls of sclerophyllous leaves accounts for little of the variation in photosynthetic nitrogen-use efficiency. *Plant, Cell & Environment* 32: 259–270.

Higgins SI, Langan L, Scheiter S. 2014. Progress in DGVMs: a comment on "Impacts of trait variation through observed trait–climate relationships on performance of an Earth system model: a conceptual analysis" by Verheijen et al. (2013). *Biogeosciences Discuss* 11: 4483–4492.

Hijmans RJ, Cameron SE, Parra JL, Jones PG, Jarvis A. 2005. Very high resolution interpolated climate surfaces for global land areas. *International Journal of Climatology* 25: 1965–1978.

Hoefnagel MHN, Atkin OK, Wiskich JT. 1998. Interdependence between chloroplasts and mitochondria in the light and the dark. *Biochimica Et Biophysica Acta-Bioenergetics* 1366: 235–255.

Huntingford C, Zelazowski P, Galbraith D, Mercado LM, Sitch S, Fisher R, Lomas M, Walker AP, Jones CD, Booth BBB et al. 2013. Simulated resilience of tropical rainforests to CO_2-induced climate change. *Nature Geoscience* 6: 268–273.

Hurry V, Igamberdiev AU, Keerberg O, Pärnik TR, Atkin OK, Zaragoza-Castells J, Gardeström P. 2005. Respiration in photosynthetic cells: gas exchange components, interactions with photorespiration and the operation of mitochondria in the light. In: Lambers H, Ribas-Carbó M, eds. *Advances in photosynthesis and respiration.* Dordrecht, the Netherlands: Kluwer Academic, 43–61.

IPCC. 2013. *Climate Change 2013: the physical science basis.* Cambridge, UK & New York, NY, USA: Cambridge University Press.

Kamaluddin M, Grace J. 1993. Growth and photosynthesis of tropical forest tree seedlings (*Bischofia javanica* Blume) as influenced by a change in light availability. *Tree Physiology* 13: 189–201.

Kattge J, Díaz S, Lavorel S, Prentice IC, Leadley P, Bönisch G, Garnier E, Westoby M, Reich PB, Wright IJ et al. 2011. TRY – a global database of plant traits. *Global Change Biology* 17: 2905–2935.

King AW, Gunderson CA, Post WM, Weston DJ, Wullschleger SD. 2006. Plant respiration in a warmer world. *Science* 312: 536–537.

Kloeppel BD, Abrams MD. 1995. Ecophysiological attributes of the native *Acer saccharum* and the exotic *Acer platanoides* in urban oak forests in Pennsylvania, USA. *Tree Physiology* 15: 739–746.

Kloeppel BD, Abrams MD, Kubiske ME. 1993. Seasonal ecophysiology and leaf morphology of four successional Pennsylvania barrens species in open versus understory environments. *Canadian Journal of Forest Research* 23: 181–189.

Kok B. 1948. A critical consideration of the quantum yield of *Chlorella*-photosynthesis. *Enzymologia* 13: 1–56.

Krömer S. 1995. Respiration during photosynthesis. *Annual Review of Plant Physiology & Plant Molecular Biology* 46: 45–70.

Kruse J, Rennenberg H, Adams MA. 2011. Steps towards a mechanistic understanding of respiratory temperature responses. *New Phytologist* 189: 659–677.

Lambers H. 1985. Respiration in intact plants and tissues: its regulation and dependence on environmental factors, metabolism and invaded organisms. In: Douce R, Day DA, eds. *Encyclopedia of plant physiology, vol. 18.* New York, NY, USA: Springer-Verlag, 417–473.

Larigauderie A, Körner C. 1995. Acclimation of leaf dark respiration to temperature in alpine and lowland plant species. *Annals of Botany* 76: 245–252.

Leuzinger S, Thomas RQ. 2011. How do we improve Earth system models? Integrating Earth system models, ecosystem models, experiments and long-term data. *New Phytologist* 191: 15–18.

Loveys BR, Atkinson LJ, Sherlock DJ, Roberts RL, Fitter AH, Atkin OK. 2003. Thermal acclimation of leaf and root respiration: an investigation comparing inherently fast- and slow-growing plant species. *Global Change Biology* 9: 895–910.

Machado JL, Reich PB. 2006. Dark respiration rate increases with plant size in saplings of three temperate tree species despite decreasing tissue nitrogen and nonstructural carbohydrates. *Tree Physiology* 26: 915–923.

Meir P, Kruijt B, Broadmeadow M, Barbosa E, Kull O, Carswell F, Nobre A, Jarvis PG. 2002. Acclimation of photosynthetic capacity to irradiance in tree canopies in relation to leaf nitrogen concentration and leaf mass per unit area. *Plant, Cell & Environment* 25: 343–357.

Meir P, Levy PE, Grace J, Jarvis PG. 2007. Photosynthetic parameters from two contrasting woody vegetation types in West Africa. *Plant Ecology* 192: 277–287.

Metcalfe DB, Lobo-do-Vale R, Chaves MM, Maroco JP, Aragao L, Malhi Y, Da Costa AL, Braga AP, Goncalves PL, De Athaydes J et al. 2010. Impacts of experimentally imposed drought on leaf respiration and morphology in an Amazon rain forest. *Functional Ecology* 24: 524–533.

Mitchell KA, Bolstad PV, Vose JM. 1999. Interspecific and environmentally induced variation in foliar dark respiration among eighteen southeastern deciduous tree species. *Tree Physiology* 19: 861–870.

Miyazawa S, Satomi S, Terashima I. 1998. Slow leaf development of evergreen broad-leaved tree species in Japanese warm temperate forests. *Annals of Botany* 82: 859–869.

Mooney HA. 1963. Physiological ecology of coastal, subalpine, and alpine populations of *Polygonum bistortoides*. *Ecology* 44: 812–816.

Mooney HA, Field C, Gulmon SL, Rundel P, Kruger FJ. 1983. Photosynthetic characteristic of South African sclerophylls. *Oecologia* 58: 398–401.

Niinemets U. 1999. Components of leaf dry mass per area – thickness and density – alter leaf photosynthetic capacity in reverse directions in woody plants. *New Phytologist* 144: 35–47.

Noguchi K, Yoshida K. 2008. Interaction between photosynthesis and respiration in illuminated leaves. *Mitochondrion* 8: 87–99.

Oberbauer SF, Strain BR. 1985. Effects of light regime on the growth and physiology of *Pentaclethra macroloba* (Mimosaceae) in Costa Rica. *Journal of Tropical Ecology* 1: 303–320.

Oberbauer SF, Strain BR. 1986. Effects of canopy position and irradiance on the leaf physiology and morphology of *Pentaclethra macroloba* (Mimosaceae). *American Journal of Botany* 73: 409–416.

Oleksyn J, Modrzynski J, Tjoelker MG, Zytkowiak R, Reich PB, Karolewski P. 1998. Growth and physiology of *Picea abies* populations from elevational transects: common garden evidence for altitudinal ecotypes and cold adaptation. *Functional Ecology* 12: 573–590.

Ow LF, Whitehead D, Walcroft AS, Turnbull MH. 2010. Seasonal variation in foliar carbon exchange in *Pinus radiata* and *Populus deltoides*: respiration acclimates fully to changes in temperature but photosynthesis does not. *Global Change Biology* 16: 288–302.

Penning de Vries FWT. 1975. The cost of maintenance processes in plant cells. *Annals of Botany* 39: 77–92.

Piao SL, Luyssaert S, Ciais P, Janssens IA, Chen AP, Cao C, Fang JY, Friedlingstein P, Luo YQ, Wang SP. 2010. Forest annual carbon cost: a global-scale analysis of autotrophic respiration. *Ecology* 91: 652–661.

Pinheiro J, Bates D, DebRoy S, Sarkar D and the R Development Core Team 2012. *nlme: linear and nonlinear mixed effects models.* R package version 3.1–105. URL http://www.r-project.org.

Poorter H, Niinemets U, Poorter L, Wright IJ, Villar R. 2009. Causes and consequences of variation in leaf mass per area (LMA): a meta-analysis. *New Phytologist* 182: 565–588.

Poorter L, Bongers F. 2006. Leaf traits are good predictors of plant performance across 53 rain forest species. *Ecology* 87: 1733–1743.

Prentice IC, Cowling SA. 2013. Dynamic global vegetation models. In: Levin SA, ed. *Encyclopedia of biodiversity, 2nd edn.* Waltham, MA, USA: Academic Press, 670–689.

Prentice IC, Farquhar GD, Fasham MJR, Goulden ML, Heimann M, Jaramillo VJ, Kheshi HS, Le Quere C, Scholes RJ, Wallace DWR. 2001. The carbon cycle and atmospheric carbon dioxide. In: Houghton JT, Ding Y, Griggs DJ, Noguer M, van der Linden PJ, Dai X, Maskell K, Johnson CA, eds. *Climate Change 2001: the scientific basis. Contribution of Working Group I to the third assessment report of the Intergovernmental Panel on Climate Change.* Cambridge, UK: Cambridge University Press, 183–237.

R Development Core Team 2011. *R: A language and environment for statistical computing.* Vienna, Austria: R foundation for Statistical computing, URL http://www.r-project.org.

Reich PB, Oleksyn J. 2004. Global patterns of plant leaf N and P in relation to temperature and latitude. *Proceedings of the National Academy of Sciences, USA* 101: 11001–11006.

Reich PB, Tjoelker MG, Machado JL, Oleksyn J. 2006. Universal scaling of respiratory metabolism, size and nitrogen in plants. *Nature* 439: 457–461.

Reich PB, Tjoelker MG, Pregitzer KS, Wright IJ, Oleksyn J, Machado JL. 2008. Scaling of respiration to nitrogen in leaves, stems and roots of higher land plants. *Ecology Letters* 11: 793–801.

Reich PB, Walters MB, Ellsworth DS, Vose JM, Volin JC, Gresham C, Bowman WD. 1998a. Relationships of leaf dark respiration to leaf nitrogen, specific leaf area and leaf life-span: a test across biomes and functional groups. *Oecologia* 114: 471–482.

Reich PB, Walters MB, Tjoelker MG, Vanderklein D, Buschena C. 1998b. Photosynthesis and respiration rates depend on leaf and root morphology and nitrogen concentration in nine boreal tree species differing in relative growth rate. *Functional Ecology* 12: 395–405.

Ryan MG. 1995. Foliar maintenance respiration of subalpine and boreal trees and shrubs in relation to nitrogen content. *Plant, Cell & Environment* 18: 765–772.

Scheiter S, Langan L, Higgins SI. 2013. Next-generation dynamic global vegetation models: learning from community ecology. *New Phytologist* 198: 957–969.

Schulze ED, Kelliher FM, Körner C, Lloyd J, Leuning R. 1994. Relationships among maximum stomatal conductance, ecosystem surface conductance, carbon assimilation rate, and plant nitrogen nutrition – a global ecology scaling exercise. *Annual Review of Ecology and Systematics* 25: 629–660.

Schwalm CR, Williams CA, Schaefer K, Anderson R, Arain MA, Baker I, Barr A, Black TA, Chen GS, Chen JM *et al.* 2010. A model-data intercomparison of CO_2 exchange across North America: results from the North American Carbon Program site synthesis. *Journal of Geophysical Research: Biogeosciences* 115: G00H05, doi: 10.1029/2009jg001229.

Searle SY, Thomas S, Griffin KL, Horton T, Kornfeld A, Yakir D, Hurry V, Turnbull MH. 2011. Leaf respiration and alternative oxidase in field-grown alpine grasses respond to natural changes in temperature and light. *New Phytologist* 189: 1027–1039.

Semikhatova OA, Gerasimenko TV, Ivanova TI. 1992. Photosynthesis, respiration, and growth of plants in the Soviet Arctic. In: Chapin FS, Jefferies RL, Reynolds JF, Shaver GR, Svoboda J, eds. *Arctic ecosystems in a changing climate.* San Diego, CA, USA: Academic Press, 169–192.

Semikhatova OA, Ivanova TI, Kirpichnikova OV. 2007. Comparative study of dark respiration in plants inhabiting arctic (Wrangel Island) and temperate climate zones. *Russian Journal of Plant Physiology* 54: 582–588.

Sendall KM, Reich PB. 2013. Variation in leaf and twig CO_2 flux as a function of plant size: a comparison of seedlings, saplings and trees. *Tree Physiology* 33: 713–729.

Sitch S, Huntingford C, Gedney N, Levy PE, Lomas M, Piao SL, Betts R, Ciais P, Cox P, Friedlingstein P *et al.* 2008. Evaluation of the terrestrial carbon cycle, future plant geography and climate-carbon cycle feedbacks using five dynamic global vegetation models (DGVMs). *Global Change Biology* 14: 2015–2039.

Sitch S, Smith B, Prentice IC, Arneth A, Bondeau A, Cramer W, Kaplan JO, Levis S, Lucht W, Sykes MT *et al.* 2003. Evaluation of ecosystem dynamics, plant geography and terrestrial carbon cycling in the LPJ dynamic global vegetation model. *Global Change Biology* 9: 161–185.

Slot M, Rey-Sánchez C, Gerber S, Lichstein JW, Winter K, Kitajima K. 2014a. Thermal acclimation of leaf respiration of tropical trees and lianas: response to experimental canopy warming, and consequences for tropical forest carbon balance. *Global Change Biology* 20: 2915–2926.

Slot M, Rey-Sánchez C, Winter K, Kitajima K. 2014b. Trait-based scaling of temperature-dependent foliar respiration in a species-rich tropical forest canopy. *Functional Ecology* 28: 1074–1086.

Slot M, Wright SJ, Kitajima K. 2013. Foliar respiration and its temperature sensitivity in trees and lianas: *in situ* measurements in the upper canopy of a tropical forest. *Tree Physiology* 33: 505–515.

Slot M, Zaragoza-Castells J, Atkin OK. 2008. Transient shade and drought have divergent impacts on the temperature sensitivity of dark respiration in leaves of *Geum urbanum*. *Functional Plant Biology* 35: 1135–1146.

Smith NG, Dukes JS. 2013. Plant respiration and photosynthesis in global-scale models: incorporating acclimation to temperature and CO_2. *Global Change Biology* 19: 45–63.

Stocker O. 1935. Assimilation und Atmung westjavanischer Tropenbäume. *Planta* 24: 402–445.

Swaine EK. 2007. *Ecological and evolutionary drivers of plant community assembly in a Bornean rain forest.* Aberdeen, UK: University of Aberdeen.

Takashima T, Hikosaka K, Hirose T. 2004. Photosynthesis or persistence: nitrogen allocation in leaves of evergreen and deciduous *Quercus* species. *Plant, Cell & Environment* 27: 1047–1054.

Tcherkez G, Boex-Fontvieille E, Mahe A, Hodges M. 2012. Respiratory carbon fluxes in leaves. *Current Opinion in Plant Biology* 15: 308–314.

Tcherkez G, Cornic G, Bligny R, Gout E, Ghashghaie J. 2005. *In vivo* respiratory metabolism of illuminated leaves. *Plant Physiology* 138: 1596–1606.

Thornton PE, Lamarque JF, Rosenbloom NA, Mahowald NM. 2007. Influence of carbon-nitrogen cycle coupling on land model response to CO_2 fertilization and climate variability. *Global Biogeochemical Cycles* 21: GB4018.

Thornton PE, Law BE, Gholz HL, Clark KL, Falge E, Ellsworth DS, Goldstein AH, Monson RK, Hollinger D, Falk M *et al.* 2002. Modeling and measuring the effects of disturbance history and climate on carbon

and water budgets in evergreen needleleaf forests. *Agricultural and Forest Meteorology* 113: 185–222.

Tjoelker MG, Craine JM, Wedin D, Reich PB, Tilman D. 2005. Linking leaf and root trait syndromes among 39 grassland and savannah species. *New Phytologist* 167: 493–508.

Tjoelker MG, Oleksyn J, Lorenc-Plucinska G, Reich PB. 2009. Acclimation of respiratory temperature responses in northern and southern populations of *Pinus banksiana*. *New Phytologist* 181: 218–229.

Tjoelker MG, Oleksyn J, Reich PB. 1999. Acclimation of respiration to temperature and CO_2 in seedlings of boreal tree species in relation to plant size and relative growth rate. *Global Change Biology* 5: 679–691.

Tjoelker MG, Oleksyn J, Reich PB. 2001. Modelling respiration of vegetation: evidence for a general temperature-dependent Q_{10}. *Global Change Biology* 7: 223–230.

Townsend AR, Cleveland CC, Asner GP, Bustamante MMC. 2007. Controls over foliar N : P ratios in tropical rain forests. *Ecology* 88: 107–118.

Turnbull MH, Tissue DT, Griffin KL, Richardson SJ, Peltzer DA, Whitehead D. 2005. Respiration characteristics in temperate rainforest tree species differ along a long-term soil-development chronosequence. *Oecologia* 143: 271–279.

UNEP. 1997. *World atlas of desertification*. London, UK: United Nations Environment Programme.

Veneklaas EJ, Poot P. 2003. Seasonal patterns in water use and leaf turnover of different plant functional types in a species-rich woodland, South-western Australia. *Plant and Soil* 257: 295–304.

Verheijen LM, Brovkin V, Aerts R, Bonisch G, Cornelissen JHC, Kattge J, Reich PB, Wright IJ, van Bodegom PM. 2013. Impacts of trait variation through observed trait–climate relationships on performance of an Earth system model: a conceptual analysis. *Biogeosciences* 10: 5497–5515.

Wager HG. 1941. On the respiration and carbon assimilation rates of some arctic plants as related to temperature. *New Phytologist* 40: 1–19.

Warton DI, Duursma RA, Falster DS, Taskinen S. 2012. SMART 3-an R package for estimation and inference about allometric lines. *Methods in Ecology and Evolution* 3: 257–259.

Warton DI, Wright IJ, Falster DS, Westoby M. 2006. Bivariate line-fitting methods for allometry. *Biological Reviews* 81: 259–291.

Weerasinghe LK, Creek D, Crous KY, Xiang S, Liddell MJ, Turnbull MH, Atkin OK. 2014. Canopy position affects the relationships between leaf respiration and associated traits in a tropical rainforest in Far North Queensland. *Tree Physiology* 34: 564–584.

Whitehead D, Griffin KL, Turnbull MH, Tissue DT, Engel VC, Brown KJ, Schuster WSF, Walcroft AS. 2004. Response of total night-time respiration to differences in total daily photosynthesis for leaves in a *Quercus rubra* L. canopy: implications for modelling canopy CO_2 exchange. *Global Change Biology* 10: 925–938.

Woodward FI, Lomas MR, Betts RA. 1998. Vegetation–climate feedbacks in a greenhouse world. *Philosophical Transactions of the Royal Society of London Series B-Biological Sciences* 353: 29–38.

Wright IJ, Reich PB, Atkin OK, Lusk CH, Tjoelker MG, Westoby M. 2006. Irradiance, temperature and rainfall influence leaf dark respiration in woody plants: evidence from comparisons across 20 sites. *New Phytologist* 169: 309–319.

Wright IJ, Reich PB, Westoby M. 2001. Strategy shifts in leaf physiology, structure and nutrient content between species of high- and low-rainfall and high- and low-nutrient habitats. *Functional Ecology* 15: 423–434.

Wright IJ, Reich PB, Westoby M, Ackerly DD, Baruch Z, Bongers F, Cavender-Bares J, Chapin T, Cornelissen JHC, Diemer M *et al.* 2004. The worldwide leaf economics spectrum. *Nature* 428: 821–827.

Wright IJ, Westoby M. 2002. Leaves at low versus high rainfall: coordination of structure, lifespan and physiology. *New Phytologist* 155: 403–416.

Wythers KR, Reich PB, Bradford JB. 2013. Incorporating temperature-sensitive Q_{10} and foliar respiration acclimation algorithms modifies modeled ecosystem responses to global change. *Journal of Geophysical Research: Biogeosciences* 118: 77–90.

Xiang S, Reich PB, Sun S, Atkin OK. 2013. Contrasting leaf trait scaling relationships in tropical and temperate wet forest species. *Functional Ecology* 27: 522–534.

Zaehle S, Medlyn BE, De Kauwe MG, Walker AP, Dietze MC, Hickler T, Luo Y, Wang Y-P, El-Masri B, Thornton P *et al.* 2014. Evaluation of 11 terrestrial carbon–nitrogen cycle models against observations from two temperate Free-Air CO_2 Enrichment studies. *New Phytologist* 202: 803–822.

Zagdanska B. 1995. Respiratory energy demand for protein turnover and ion transport in wheat leaves upon water deficit. *Physiologia Plantarum* 95: 428–436.

Zaragoza-Castells J, Sanchez-Gomez D, Hartley IP, Matesanz S, Valladares F, Lloyd J, Atkin OK. 2008. Climate-dependent variations in leaf respiration in a dry-land, low productivity Mediterranean forest: the importance of acclimation in both high-light and shaded habitats. *Functional Ecology* 22: 172–184.

Zomer RJ, Trabucco A, Bossio DA, Verchot LV. 2008. Climate change mitigation: a spatial analysis of global land suitability for clean development mechanism afforestation and reforestation. *Agriculture, Ecosystems & Environment* 126: 67–80.

Zotz G, Winter K. 1996. Diel patterns of CO_2 exchange in rainforest canopy plants. In: Mulkey SS, Chazdon RL, Smith AP, eds. *Tropical forest plant ecophysiology*. New York, NY, USA: Chapman & Hall, 89–113.

Zuur AF, Ieno EN, Walker N, Saveliev AA, Smith GM. 2009. *Mixed effects models and extensions in ecology with R*. New York, NY, USA: Springer Science and Business Media.

Supporting Information

Additional supporting information may be found in the online version of this article.

Fig. S1 Comparison of R_{dark}^{25}, calculated assuming either a fixed Q_{10} or a T-dependent Q_{10}.

Fig. S2 Relationships between leaf structural/chemical composition traits and TWQ.

Fig. S3 R_{dark}–aridity index relationships, excluding data from a high-rainfall site in New Zealand.

Fig. S4 R_{dark}–MMT relationships for those sites where the month of measurement was known.

Fig. S5 Testing key assumptions for mixed-effects models – homogeneity and normality.

Fig. S6 Model validation graphs for the area-based mixed-effects model.

Fig. S7 Standardized residuals against fitted values for variables not used in the mixed model.

Fig. S8 Dotchart of the area-based mixed model's random intercepts by family.

Fig. S9 Dotchart of the area-based mixed model's random intercepts by site.

Table S1 Details on unpublished databases used in the global database of R_{dark}

Table S2 Details on published databases used in the global database of R_{dark}

Table S3 Standardized major axis regression slopes for relationships in Figs 5, 6

Table S4 Comparison of mixed-effects models with area-based R_{dark}^{25} as the response variable

Table S5 Comparison of mixed-effects models using different plant functional type (PFT) classifications, with R_{dark}^{25} as the response variable

Methods S1 Sampling methods and measurements protocols for previously unpublished data.

Methods S2 Details on methodology used to temperature normalize respiration rates.

Please note: Wiley Blackwell are not responsible for the content or functionality of any supporting information supplied by the authors. Any queries (other than missing material) should be directed to the *New Phytologist* Central Office.

About *New Phytologist*

- *New Phytologist* is an electronic (online-only) journal owned by the New Phytologist Trust, a **not-for-profit organization** dedicated to the promotion of plant science, facilitating projects from symposia to free access for our Tansley reviews.

- Regular papers, Letters, Research reviews, Rapid reports and both Modelling/Theory and Methods papers are encouraged. We are committed to rapid processing, from online submission through to publication 'as ready' via *Early View* – our average time to decision is <26 days. There are **no page or colour charges** and a PDF version will be provided for each article.

- The journal is available online at Wiley Online Library. Visit **www.newphytologist.com** to search the articles and register for table of contents email alerts.

- If you have any questions, do get in touch with Central Office (np-centraloffice@lancaster.ac.uk) or, if it is more convenient, our USA Office (np-usaoffice@lancaster.ac.uk)

- For submission instructions, subscription and all the latest information visit **www.newphytologist.com**